

AEROSPACE ENGINEERING — GREVA — AIRPLANE DESIGN

CONCEPTUAL DESIGN OF AN ELECTRICAL AEROBATIC AIRCRAFT



Group 11

Álvaro Casas Martínez Adam El Ghaib Bourgine

Álvaro Peregrín Pastor David Roldan Vilardell

Professor

Ester Comellas Sanfeliu



UNIVERSITAT POLITÈCNICA DE CATALUNYA

JANUARY 24, 2024



Abstract

Nowadays, the willingness to become environmentally friendly has gained much importance. However, not all fields have the same opportunities to adapt to this movement. Mainly, due to the complexity and feasibility that entails introducing big changes. In this project, a preliminary design of an aerobatic electric-powered aircraft is going to be proposed. Currently, this kind of airplane already exists, but, because of its narrow range of applications, is quite an unpopular and more expensive option for customers. In this study, some improvements to the performance of the present available electric-driven aerobatic planes are analyzed. The methodology followed for the design is the one proposed by M.H Sadraey in his book “Aircraft Design A Systems Engineering Approach” [1].

Key words: Aerobatic, Aircraft, Plane, Electric, Design, Performance, Environment, Sadraey.

Contents

1	Introduction	1
1.1	Objective	1
1.2	Scope	1
1.3	Motivation	1
1.4	Requirements	2
1.5	Reference aircraft	3
1.5.1	Xtremeair Sbach 342 (XA42)	3
1.5.2	Extra 330LE	3
1.5.3	Rolls-Royce ACCEL	4
1.5.4	Extra 300L	4
1.5.5	SUKHOI SU29	5
1.5.6	Pitts S-2C	5
2	Market study	7
2.1	State of the art	7
2.2	Market opportunities	8
2.3	Reference aircraft data	9
3	General configuration	10
3.1	Fuselage	10
3.2	Wing	10
3.3	Tail	10
3.4	Landing gear	11
3.5	Powerplant	11
4	Weight study	12
4.1	Maximum Take-Off Mass (MTOM)	12
4.2	Payload	12
4.3	Maximum Take-Off Mass - Approximation	12
5	Design point	15
5.1	Stall speed	15
5.2	Maximum speed	15
5.3	Maximum rate of climb	16
5.4	Take-off run	16
5.5	Ceiling	16
5.6	Variables chosen	16
5.7	Performance diagram	17



6 Drag coefficients estimation	19
7 Maneuver and gust diagram	22
7.1 Maneuver diagram	22
7.2 Gust diagram	23
8 Electric propulsion	25
8.1 Propeller	25
8.2 Motor and battery	27
8.3 Flight time and range	29
9 Range vs payload	32
9.1 Deduction of range vs payload	32
9.2 Calculation of range vs payload	33
10 Wing Design	34
10.1 Airfoil Selection	35
10.2 Sweep angle	37
10.3 Taper ratio & Twist angle	38
10.4 Final wing configuration	41
11 Tail design	42
11.1 Horizontal stabilizer	42
11.1.1 Tail surface	42
11.1.2 Geometric parameters	43
11.1.3 Airfoil selection	45
11.1.4 Incidence angle	45
11.2 Vertical stabilizer	45
11.2.1 Surface	45
11.2.2 Geometric parameters	46
11.2.3 Airfoil selection	47
12 Stability and control	48
12.1 Pitching stability	48
12.2 Roll momentum	51
13 Fuselage design	54
13.1 Landing Gear	54
14 Renders and drawings	56



15 Conclusions	59
Appendices	i
A Code	i
A.1 OEM & MTOM estimation	i
A.2 Performance diagram	i
A.3 Drag coefficients estimation	iv
A.4 Maneuver and gust diagram	v
A.5 Electric Propulsion	viii
A.6 Range vs payload	xi
A.7 Stability and control	xi
B Velocities calculation	xvii



1 Introduction

1.1 Objective

The objective of the project is to carry out a preliminary design of a two-seater electric aerobatic plane, in order to have an aircraft capable of being used in aerobatic competitions, exhibitions, pilot training, or recreational use.

1.2 Scope

The scope of this project:

Will include:

- ◊ Market study
- ◊ Weight study
- ◊ Selection of the design point
- ◊ Drag estimation and gust diagram
- ◊ Propeller selection and propeller-motor efficiency matching study.
- ◊ Range and autonomy study.
- ◊ Wing, tail, fuselage, and control surfaces design.
- ◊ Stability study
- ◊ Preliminary 3D CAD model.

Will not include:

- ◊ FEM or CFD analysis
- ◊ Landing gear design
- ◊ Avionics design
- ◊ Mechanical control system in between the pilot and control surfaces
- ◊ Manufacturing of the aircraft
- ◊ Economic feasibility of the project
- ◊ Integration and power distribution of all the electronic devices.

1.3 Motivation

Nowadays, the desire to reduce global warming effects has become our duty. It is a fact that fuel-propelled aerobatic aircraft pollute due to their high power requirements and their propulsion efficiencies, rounding the 40%. Moreover, there are some complaints about acoustic disturbance. As *Impact of the electric propulsion on aircraft noise* [2] study shows, aircraft electrification is capable of reducing up to 14.5 dB, in addition, electric engines increase efficiency to the 90% [3]. Furthermore, aerobatic recreational flights usually last about 30 minutes, and competitions not much more than 1 minute at maximum power conditions. With all this in mind, it has been decided to use electric propulsion due to its suitability with the requirements of this project.



1.4 Requirements

The main *top level requirements* of the aircraft are the following:

- ◊ The airplane has to be environmentally friendly, that is to say, it must not use fossil fuels. The aircraft will use an electric engine to propel it.
- ◊ In order to maximize the range of applications, the aircraft must have a capacity for two people. This will make it possible to use it for teaching or recreational purposes.
- ◊ Even though average pilots can only handle +4.5g, -1.5g [4]. The structure of the aircraft has to hold a minimum of +8g, -5g forces to be capable of doing all the demanding maneuvers, maximize the range of applications, and stand out from the competition.
- ◊ The aircraft must have a flight autonomy of 30 minutes. And the plane has to land before the battery level reaches 20% of the total capacity so that the battery is well preserved, and unnecessary battery malfunctions are avoided. These values are commonly set in electric general aviation aircraft [5].
- ◊ An aerobatic aircraft has to have the capability to take off from a short distance. That is because some exhibitions and competitions occur in the middle of the city [6], where there is little space to accelerate. Thus, the take-off distance will be set to 200 m.



1.5 Reference aircraft

The design will be based, mainly, on two different aircraft, not only to take some ideas for the structure or the aerodynamics but also to have them as a benchmark.

1.5.1 Xtremeair Sbach 342 (XA42)

The XA42 is the aerobatic aircraft used in flying competitions by teams like Red Bull. It is an aerobatic two-seater plane capable of supporting more G-forces than a human being can test for a few seconds, specifically $\pm 10g$. Due to the XA42's great performance, we want to use it as an aerodynamics reference. Moreover, this aircraft could be the subject of a structural study because of its good operation.



Figure 1: Xtremeair Sbach 342. Image from [7].

1.5.2 Extra 330LE

The 330LE is one of the first electric aerobatic airplanes and the first to have a performance that can be compared to an aircraft propelled by fossil fuels. This aircraft will be a reference, especially in terms of the engine and the way that it transmits power to the propeller.



Figure 2: Extra 330LE. Image from [8].



1.5.3 Rolls-Royce ACCEL

With a battery output power of 373 kW (500 HP) continuous, and 750 kW (1,010 HP) at maximum power. The Rolls-Royce ACCEL or also called the “Spirit of Innovation” is the fastest electric airplane ever built, reaching a top speed of 622 km/h. Even though it is not designed for aerobatic purposes, it will serve us as a reference in propulsion matters.



Figure 3: Rolls-Royce ACCEL. Image from [9].

1.5.4 Extra 300L

The design of the Extra 300 is based on the Extra 230, an early 1980s monoplane with wooden wings. The Extra 300 has a fuselage of welded metal tubes covered with fiberglass and fabric. The main wing spar is made of a carbon fiber composite as is the wing surface. A symmetrical airfoil, with zero angle of incidence and zero dihedral, provides uniform flight in both normal and inverted positions. The landing gear is fixed encapsulated for improved aerodynamics using glass fiber-coated composite materials. The engine is a Lycoming AEIO-540 opposed-cylinder, fuel-injected, 224 kW engine.



Figure 4: Extra 300L. Image from [10].



1.5.5 SUKHOI SU29

The Sukhoi Su-29 is a two-seat aircraft equipped with a tandem cockpit, based on the Sukhoi Su-26MX. With it, Sukhoi wanted to cover mainly the North American market and thus develop an important source of income for US dollars.

Development began in 1990 and was based on the Su-26M. The prototype, which had not yet flown, was first exhibited at the 1991 Aérosalon in Le Bourget. The aircraft made its maiden flight on 9 August 1991 with Yevgeny Frolov in the cockpit. Two more prototypes flew in the autumn of 1991 and spring of 1992, followed shortly after by the first production aircraft.



Figure 5: SUKHOI SU29. Image from [11].

1.5.6 Pitts S-2C

The Pitts S-2C is a 2-place, single-seat biplane. It is a competition aerobatic aircraft that was designed by Curtis Pitts of the United States and first flown in 1949. The aircraft's design incorporates many advanced features such as an enclosed cockpit and interlocking control sticks to enhance safety.



Figure 6: Pitts S-2C. Image from [12].



2 Market study

2.1 State of the art

At the outbreak of World War I, military pilots were used mainly for reconnaissance work and were not expected to possess any knowledge of aerobatics. It was not until the development of successful fighter aircraft in 1915 that pilots began to engage in serious aerial combat, discovering in the process that aerobatic skills could give them a significant advantage in a dogfight.[13]

After World War I, former combat pilots continued to refine their skills. Giving rise to new ways of entertainment such as the barnstorming era. During the roaring twenties, stunt pilots performed tricks individually or in groups that were called flying circuses. Barnstorming was the first major form of civil aviation in the history of aviation[14]. While in Europe the most proficient war pilots were employed by the aircraft manufacturers, displaying their skills and the manufacturer's products at public air shows.

The first and only World Cup of aerobatics was held in Paris in June 1934, with nine entries from six countries (all European). Aerobatic events were also held in conjunction with the 1936 Olympic Games in Berlin.

After World War II, aerobatic activities started to be organized and regulated. Competitions like the Lockheed Trophy that was held annually in England from 1955 to 1965 awarded freestyle aerobatics and called the attention of the public. Afterward, the aerobatic commission of the *Fédération Aéronautique Internationale* (FAI), which is the world governing body for air sports and was founded in 1905[15], organized the World Aerobic Championships (WAC) in 1960[16], a competition that is still performed nowadays and it is the most iconic aerobatic competition in the world.

Regulations and score systems have been changing through the years, but the basic philosophy has remained constant. Each pilot is required to fly a number of individual sequences of aerobatic figures, which are scored by a panel of judges. Finally, the pilot with the highest score wins the competition.

2.2 Market opportunities

Fig. 7 shows that in the aeronautical industry, narrow-body and wide-body jet aircraft were the most produced in 2013, mainly by the aircraft manufacturers Boeing and Airbus.

However, our target will lie in turboprop aircraft specifically, on electric powered turboprops, a more environmentally-friendly option. Therefore, we aim for a relatively reduced and particular market niche.

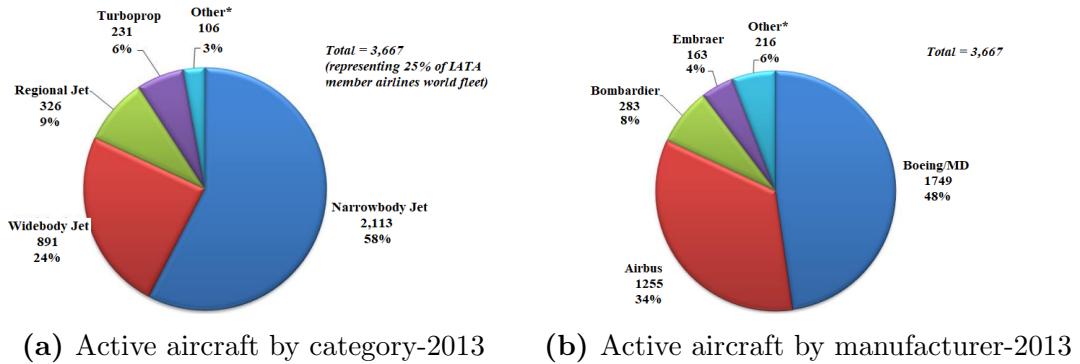


Figure 7: Market distribution in 2013. Image from [17].

Below, some of the most promising market opportunities of our design are studied.

Pilot training

According to CAE Global Academy, “The civil aviation industry will require 264,000 new pilots over the next decade. Age-based retirement and attrition combined with fleet growth are the main drivers of pilot demand”[18]. This key factor is one of the strongest arguments that give a good demand for our product. As our plane will be electric, it adds a positive thing which is the fuel saving which is of utmost importance at the moment due to the increase in fuel prices. At the same time, autonomy is affected and classes could not be longer than 40 minutes. It would therefore be ideal for practicing take-offs, landings, aerobatic techniques, and short duration flights but not so much for more extended general navigation.

Aerobic Competitions

If our design is feasible and competent, our plane could be provided to racing and aerobatic pilots in order to be used in competitions such as:

- ◊ The **FAI World Aerobatic Championships** (WAC): A competition in sport aviation organized by CIVA (Commission Internationale de Voltige Aérienne), the aerobatic commission of the FAI, the world air sports federation. The WAC was formed in 1960, replacing the freestyle Lockheed Trophy contests. And nowadays is the most important aerobatic competition in the world.



- ◊ **Air Race E:** A revolutionary form of Air Racing. It is the first ever all-electric airplane race. The future of aviation is in green energy and Air Race E is setting the marker for future developments in electric aviation with a world first airplane race never seen before.

2.3 Reference aircraft data

In order to present the data of the reference aircraft in a clearer and more synthesized way, it will be put together in a table the most important operating values.

	Extra 330LE	Sbach 342	Sukhoi su 29	Pitts S-2C	RR ACCEL	Extra 330L
Propulsion type	Electric	Fuel	Fuel	Fuel	Electric	Electric
MTOM [kg]	1000	850	1100	737	1350	952
Pax	2	2	2	2	2	2
Max Speed [km/h]	375	343	340	337	622	293
Power[kW]	260	235	268	194	373	224
Strength	-	-10,+10G	-10,+12G	-5,+6G	-	-8,+8G
Weight/Power [N/kW]	37.77	35.45	40.22	37.29	35.56	41.65
Wing Area (m^2)	10.84	11.25	12.24	11.6	6.5	10.7
W.load (N/m^2)	935.78	741.24	881.58	623.28	2037.98	872.81
Length [mm]	7500	6670	7320	5710	7000	7000
Wingspan [mm]	8000	7500	8200	6100	7300	8000
Price [€]	-	268.000	195.000	230.000	-	365.000

Table 1: Data of the reference aircraft.

As it is shown above, all the planes have more or less the same specifications, but there are two key factors in regard to the Extra 330LE. The first one is the MTOM which, despite being 100 kg less than the Sukhoi su 29, it is still very high taking into account it is practically constant throughout the flight. And the other one is the engine that has a power of 260 kW with a constant torque of 1000 Nm that goes directly to the propeller which causes a maximum speed of 375 km/h, allowing for generally better performances. Having 15 knots more is a huge difference in this type of aircraft. However, it is noteworthy to say that not always more engine power results in a better aircraft.



3 General configuration

This section will talk about the main characteristics of the aircraft, considering all the airplanes discussed in section 2.3.

3.1 Fuselage

The fuselage has two key factors, the cross-section shape and whether it is pressurized or not. According to EASA regulation CS-23, if the aircraft does not fly above 7620 m, the fuselage does not need to be pressurized. In this case, the fuselage is not pressurized because it will save money and space, which for a small aircraft it is very necessary. Because the cockpit is pressurized, the cross-section can be rectangular or circular shaped.

Lastly, other important characteristics to take into account for the fuselage design are the door and the seats. For this airplane, due to the reduced amount of space, the door will be a cockpit, that is, a door that opens from the roof of the plane instead from the side. And the two seats will be arranged in tandem configuration.

3.2 Wing

The wing is the main lifting system of the aircraft, so it is reasonable to say that is, probably, the most important part of the plane. There are many possible configurations for the wing design, but the chosen one has to fulfill the purpose of the aircraft.

Thus, the airplane will be a monoplane because there is no need to install another wing since the plane's high speed will counteract the lift deficit. The wing location will be low due to it is the most maneuverable configuration of all the possible ones. As can be seen, all the decisions have been taken thinking about maneuverability, which is essential for an aerobatic aircraft. As for the wing surface and the profile, they will be discussed further on, in sections 5 and 10, respectively.

3.3 Tail

The two types of tails considered for the design are the conventional and the T-tail. A T-tail provides some advantages like high efficiency and a safe structure because the tail is out of the regions of the wing wake, wing downwash, and wing vortices. But it has a massive disadvantage, which is the deep stall. It consists of a stall condition when the tail is set at a high angle of attack. This is not valid for an aerobatic aircraft, since it will sometimes be flying at high angles of attack.

So, the tail chosen is the conventional, as the name implies, it is the most used tail



configuration. It is simple, safe, and equilibrated.

3.4 Landing gear

The landing gear will be a fixed tripod with fairing. This decision is made thinking about the size of the plane. The retractile system uses space inside the fuselage that would be useful for the engine or the batteries. Moreover, it also adds some weight, which is not the best option for an aerobatic aircraft that will compete in races and events. Usually, the lighter this type of aircraft is, the better they perform.

3.5 Powerplant

One of the requirements of the project is that the aircraft must be eco-friendly, so it can not use any fossil fuels. The best and most plausible option is to use an electric engine and power it with electric batteries. Another option would be hydrogen fuel cells, but they are not yet a realistic option.

Nowadays, there are only two different options from where to choose. Even though the market for electric motors is rising fast, engines with high power and low volume are still in the testing phase. The options considered are the following:

	Power [hp]	Weight [kg]
Extra 330LE	348	50
RR ACCEL	500	65

Table 2: Powerplants available.



4 Weight study

4.1 Maximum Take-Off Mass (MTOM)

MTOM is defined as the maximum mass that an aircraft can hold for its take-off. This includes the operational empty mass (OEM), the payload (PL), and the fuel mass (FM). As Voltic will be electric propelled, the FM is not going to be part of the study, therefore, a zero value for the FM is assumed. Taking this into account, MTOM is going to be calculated as:

$$MTOM = PL + OEM \rightarrow MTOM \geq \frac{PL}{1 - \frac{OEM}{MTOM}} \quad (1)$$

4.2 Payload

According to the FAA, an adult person weighs 89 kg [19]. So if the aircraft will carry a maximum of two people, our payload will be around 200 kg. Allowing people to bring 11 kg for any equipment or specific necessities.

4.3 Maximum Take-Off Mass - Approximation

Due to the lack of references for electric aerobatic aircraft, it is going to be a complicated task to find accurate mass parameters. The main theoretical support is going to be the process used to convert Extra 300L to an electric aircraft, Extra 330LE. Although the most correct process would be to use electric aircraft as a reference, it will be made a preliminary estimation using the aerobatic reference planes which are more in line with the Voltics concept, then these values are going to be corrected using a similar electrification process as Extra 300L did.

Putting together mass parameters of the mentioned aircraft:

Aircraft	MTOM [kg]	OEM [kg]
Sbach 342	850	670
Sukhoi	1100	760
Pitts	737	521
Extra 300	952	628

Table 3: OEM and MTOM.

Analyzing the values from Table 3, a linear correlation between OEM and MTOM may exist, so the first MTOM approach will be made by using a method that allows defining

the ratio of OEM to MTOM. With this in mind, plotting OEM against MTOM can be very useful for estimating these Voltic parameters.

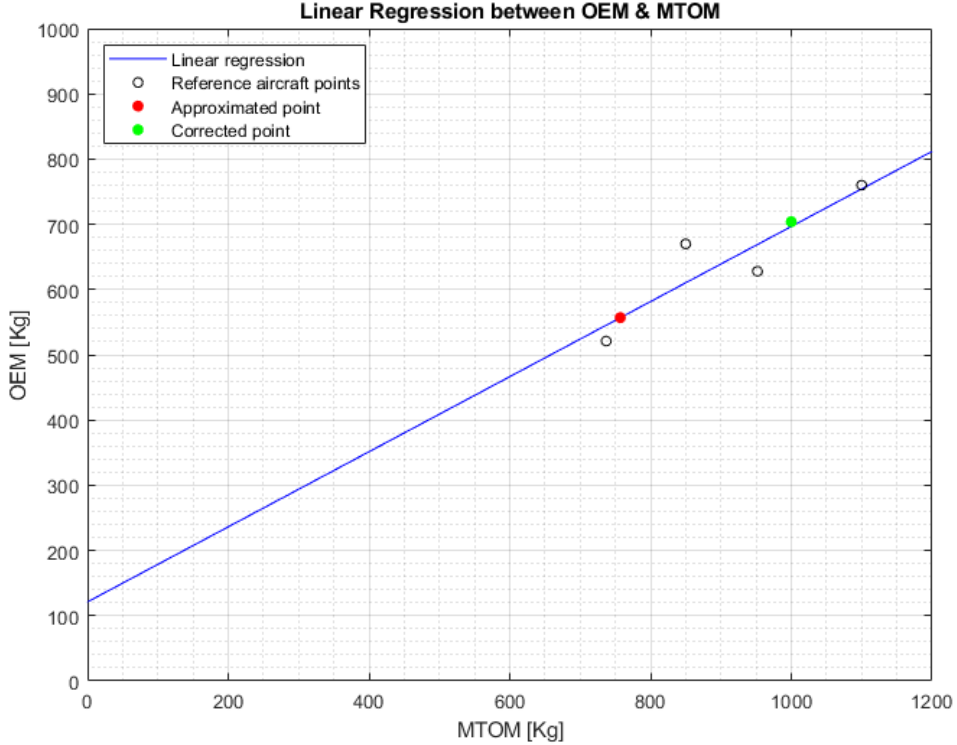


Figure 8: Linear regression relation between OEM against MTOM.

$$OEM = 0.576 \cdot MTOM + 121.173 \quad (2)$$

Note that the linear regression from Figure 8 does not contain (0,0) point, which should be a result of the reality. The main reason for that is that this approximation has been done for the 700 to 1100 MTOM range.

Solving equations 1 and 2 with $PL = 200 \text{ kg}$ results in $MTOM \geq 757 \text{ kg}$, therefore $OEM \approx 557$. This result has to be taken as an illustrative value since we are considering non-electric aerobatic planes, thus, this may cause some distortion in the linear approximation.

As this result is not as accurate as it is ought to, it is going to be used the converting process of Extra 300L to EXTRA 330LE as a reference, which has replaced fuel with electric propulsion.

Extra 300L OEMs is about 653 kg [20], as the engine mass of the aircraft is 199 kg [21], Extra 300L OEMs is rounding 450 kg without the engines. Going for the Extra 330 LE parameters, it is going to be added the engine (50 kg), so now the aircraft is rounding the



500 kg. With this in mind, as Extra 330LE MTOM \approx 1000 kg, it can be considered that half of the MTOM is designated for payload and batteries.

Studying now Voltic's case, OEM = 557 kg, which is going to be subtracted 199 kg from the fuel engine and added 50 kg due to the electric engine. Thus, OEM = 408 kg. At this moment, it has to be added the battery and payload mass. To approximate this mass, it is going to be used values from Extra 330LE. As the Extra 300L and 330LE OEM's follows Equation 3, it can be computed the mass from the transformation as 4.

$$OEM_{330LE} - M_{e,330LE} = OEM_{300L} - M_{e,300L} \quad (3)$$

Where M_e is the mass corresponding to each engine.

$$MTOW_{LE} - OEM_{330LE} = PL + \Delta Battery \quad (4)$$

$$MTOW_{LE} - (OEM_{300E} - M_{e,300L} + M_{e,330LE}) = PL + \Delta Battery$$

Replacing all the values results in $PL + \Delta Battery = 496$ kg. Finally, MTOM = $408 + 496 = 904$ kg. This result may be a good mass estimation, but, due to the fact that the aircraft should be willing to withstand more g forces than Extra LE does, it is going to be considered MTOM = 1000 kg. This fact will also be very helpful to have a great security margin. This result means that now $MTOM_{corrected} - MTOM_{initial} = 96$ kg. For this first estimation this kg increment is going to be destined to battery mass, so $PL + \Delta Battery = 592$, as $PL = 200$, 392 kg is going to be the battery mass.

It is important to note that by doing this estimation there is a percentage of error because of the use of non-electric propelled aircraft, nevertheless with the correction done it might be a good approximation for a first iteration. As long as the different parts of the project start being fixed, these values are going to be adjusted.

Finally, a table summarizing the results:

Mass parameter	Value [kg]
MTOM	1000
OEM	496
Payload	200
Battery	392

Table 4: Parameters from Voltic.



5 Design point

The determination of the design point consists in finding an engine and a wing surface that fit all the parameters of the aircraft. The engine and the wing surface will be calculated depending on the MTOW, which has been calculated in section 4.

The method followed is analytical, using *Mohammad H. Sadraey. Aircraft design: A systems engineering approach* [1], that uses the following variables to estimate the design point:

- ◊ Stall speed (V_s)
- ◊ Maximum speed (V_{max})
- ◊ Maximum rate of climb (ROC_{max})
- ◊ Take-off run (S_{TO})
- ◊ Ceiling (h_c)

From the variables shown above, it will be possible to calculate the ratio W/P , because it is a propeller-driven aircraft, according to the wing load (W/S). All the restrictions create an area in which the design point is found. The values used in the following sections are specified and justified in section 5.6

5.1 Stall speed

The stall speed (V_s) is the minimum speed that allows the aircraft to do a straight level flight. In this case, when plotting the function W/P vs W/S , it will be a vertical line because it does not depend on the W/P ratio and the design point must be at the left of the line.

$$\left(\frac{W}{S}\right)_{V_s} = \frac{1}{2}\rho V_s^2 C_{L_{max}} \quad (5)$$

5.2 Maximum speed

The maximum speed (V_{max}) is one of the most important parameters for an aerobatic aircraft because it could define the result of a race, for example. Now, the design point will be below the curve.

$$\left(\frac{W}{P_{SL}}\right)_{V_{max}} = \frac{\eta_P}{\frac{1}{2}\rho_o V_{max}^3 C_{D_o} \left(\frac{1}{\frac{W}{S}}\right) + \frac{2K}{\rho V_{max}} \left(\frac{W}{S}\right)} \quad (6)$$



5.3 Maximum rate of climb

The rate of climb (ROC) is the capacity of the airplane to gain altitude in a certain amount of time. For this curve, the design point will be below it.

$$\left(\frac{W}{P}\right)_{ROC} = \frac{1}{\frac{ROC}{\eta_P} + \sqrt{\frac{2}{\rho \sqrt{\frac{3C_{D_o}}{K}}} \left(\frac{W}{S}\right) \left(\frac{1.155}{(L/D)_{max} \eta_P}\right)}} \quad (7)$$

5.4 Take-off run

This is another critical requirement because this type of airplane has to be able to take off from somewhere that is not a runway and there is not always much space. Like in the other cases, the design point is below the curve.

$$\left(\frac{W}{P}\right)_{S_{TO}} = \frac{1 - \exp\left(0.6\rho g C_{D_G} S_{TO} \frac{1}{W/S}\right)}{\mu - \left(\mu + \frac{C_{D_G}}{C_{L_R}}\right) \left[\exp\left(0.6\rho g C_{D_G} S_{TO} \frac{1}{W/S}\right)\right]} \frac{\eta_P}{V_{TO}} \quad (8)$$

5.5 Ceiling

The ceiling flight sets the highest altitude where the aircraft can climb by its own engine and have sustained flight. The lack of information about electric aircraft forced us to use the service ceiling as the reference ceiling, which has a $ROC = 0.508 \text{ m/s}$. The design point must be below the curve.

$$\left(\frac{W}{P_{SL}}\right)_C = \frac{\sigma_C}{\frac{ROCC_C}{\eta_P} + \sqrt{\frac{2}{\rho \sqrt{\frac{3C_{D_o}}{K}}} \left(\frac{W}{S}\right) \left(\frac{1.155}{(L/D)_{max} \eta_P}\right)}} \quad (9)$$

5.6 Variables chosen

All the equations shown above, from 5 to 9, use parameters that have to be estimated in order to develop the plot. In this case, like the equations, the values of the parameters are based on the Sadraey book [1], or from data of reference aircraft.

Parameters	Value	Unit
V_{stall}	30	m/s
V_{max}	98	m/s
Take-off run	200	m
ROC	12.7	m/s
Ceiling (service)	3500	m
ρ_{flight}	1.07	kg/m^3
AR	5.5	-
e	0.7	-
η	0.8	-
CL_{max}	2	-
CD_0	0.03	-
CL_{flapTO}	0.5	-
CL_c	0.3	-
L/D _{max}	10	-

Table 5: Estimated parameters.

5.7 Performance diagram

Plotting all the mentioned parameters in one graphic results in Figure 9.

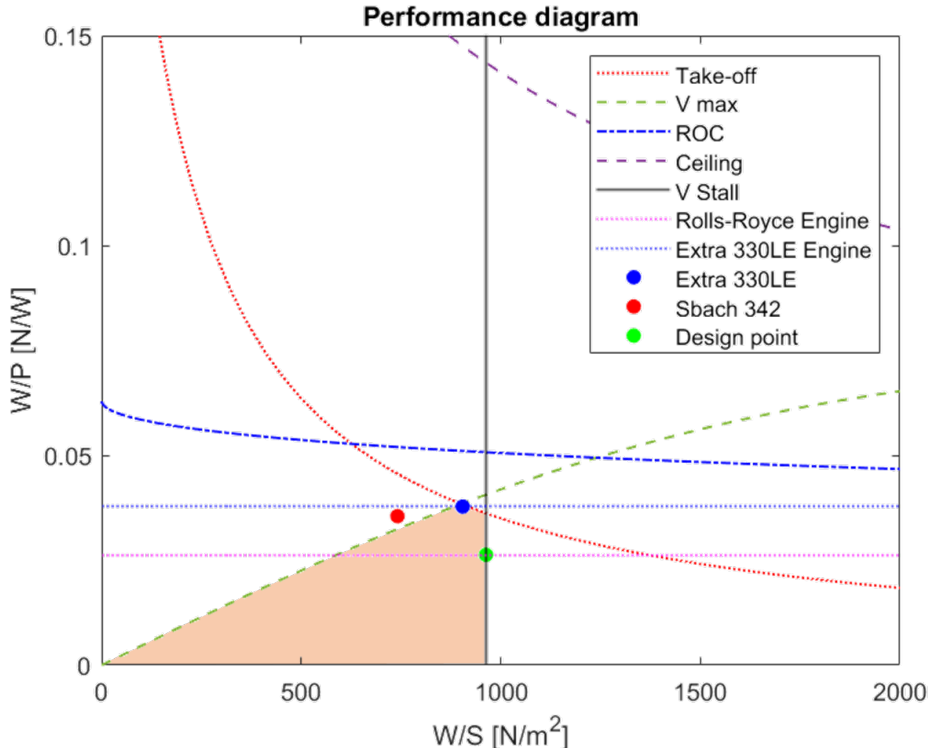
**Figure 9:** Design point plot of a prop-driven aircraft.



Figure 9 shows the closed area which provides us with all the points where the design point serves our requirements. It can be seen that one of the reference aircraft's design points drops out of this area, however, that is not a problem because of its proximity to the design point area. Note that not all the curves mentioned in this section are closing the area, this means that not all our *TLR* are restricting the aircraft's performance. In particular, *Ceiling* and *ROC* are not restricting, nevertheless *Take-off*, *V Stall* and *V max* curves are marking this area.

One important thing is that the design point has been chosen based on the possible engines that had been taken into account. As it can be seen in Figure 9, the engine chosen is the one that runs the Rolls-Royce ACCEL. It has a power of 373 kW which, with $MTOM = 1000 \text{ kg}$, the final weight-power ratio is 26.3 N/W . This has been the final election because if it were chosen Extra's engine, both planes would be very similar. So to stand out from the competition, the best way is with one of the fastest electric engines ever built.

As for the wing loading, it has been set to a value of 963 N/m^2 because is the way to maximize the speed. Although it is true that with more wing loading maneuverability decreases, it can be compensated with power, and in this case, it is the best possible scenario. With this value, the wing surface can be sized.

$$S = \frac{W}{W/S} = 10.18 \text{ m}^2 \quad (10)$$

To sum up, it can be seen that Voltic is managing to reach the *TLRs*, even willing to outperform the benchmark aircraft in some fields due to its power plant. The wing loading, 963 N/m^2 , is a bit higher than Extra 330LE, but this should not be a problem due to the fact that there is a small difference. As the wing loading, and the wing area is very similar to Extra 330LE, this aircraft might be a good geometric and structural reference for the wing, nevertheless, differs a little from other reference aircraft, but this should not be a problem due to the small difference between wing area and the difference existing between propulsive characteristics. Finally, the weight-power ratio is the parameter that differs the most from the reference aircraft. The weight-power ratio is highly lower compared to reference aircraft, this means that for similar aircraft weights, Voltic will have much more power to perform the same maneuvers.



6 Drag coefficients estimation

As various parameters of the wing configuration are still to be determined, the most appropriate method to estimate the drag coefficients is the one proposed by Sadraey. This method is based on statistical techniques and makes use of the aircraft performances which are already known.

For a propelled driven aircraft the zero drag coefficient can be calculated as:

$$C_{D_0} = \frac{2 \frac{P_{SL_{max}} \cdot \eta_P}{V_{max}} - \frac{2kW^2}{\rho o V_{max}^2 S}}{\rho o V_{max}^2 S} \quad (11)$$

Where k is the induced drag coefficient and can be obtained as:

$$k = \frac{1}{\pi e A R}$$

According to Table 5.8 of [1], the aspect ratio for general aviation aircraft ranges between 5 and 9. This can be seen in our reference planes. The higher the aspect ratio the more efficient the wing is as it behaves more like a 2D airfoil. Nonetheless, increasing the AR also increases the bending moment sustained by the root wing, causing it to be heavier or more heavily reinforced.

	Extra 330LE	Sbach 342	Sukhoi su 29	RR ACCEL
AR	5.9	6	5.5	8

Table 6: Aspect ratio of some reference planes.

It can be noticed that the RR Accel unlike the other aircraft references is a racing plane so it can afford to have a higher AR as it faces lower bending moments. One top level requirement established for this project is the capability of the plane to support accelerations up to 8g. To be conservative, it has been decided an $AR = 5.5$ for this initial estimation, mainly based on the reference aircraft.

The Oswald efficiency factor is estimated using this formula proposed in Raymer[22].

$$e = 1.78 \cdot (1 - 0.045 \cdot AR^{0.68}) - 0.64$$

The engine power and the wing surface are estimated knowing the MTOW and the design point that determines the wing loading and the power loading. These values are known from section 5.



$$S = W_{TO}/(\frac{W}{S})_d \quad (12)$$

$$P = W_{TO}/(\frac{W}{P})_d \quad (13)$$

The plane of this project is electrically propelled so the take-off and the landing weights are the same since no fuel is consumed.

Assuming:

$$W = W_{TO} \text{ N} ; V_{max} = 1.2V_c ; V_c = 81.67 \text{ m/s} ; \rho = 1.07 \text{ kg/m}^3 ; \rho_o = 1.225 \text{ kg/m}^3 ;$$

$$\sigma = \frac{\rho}{\rho_o} ; \eta_P = 0.8$$

The aircraft's polar estimation is:

$$C_D = 0.048379 + 0.065418 \cdot CL^2$$

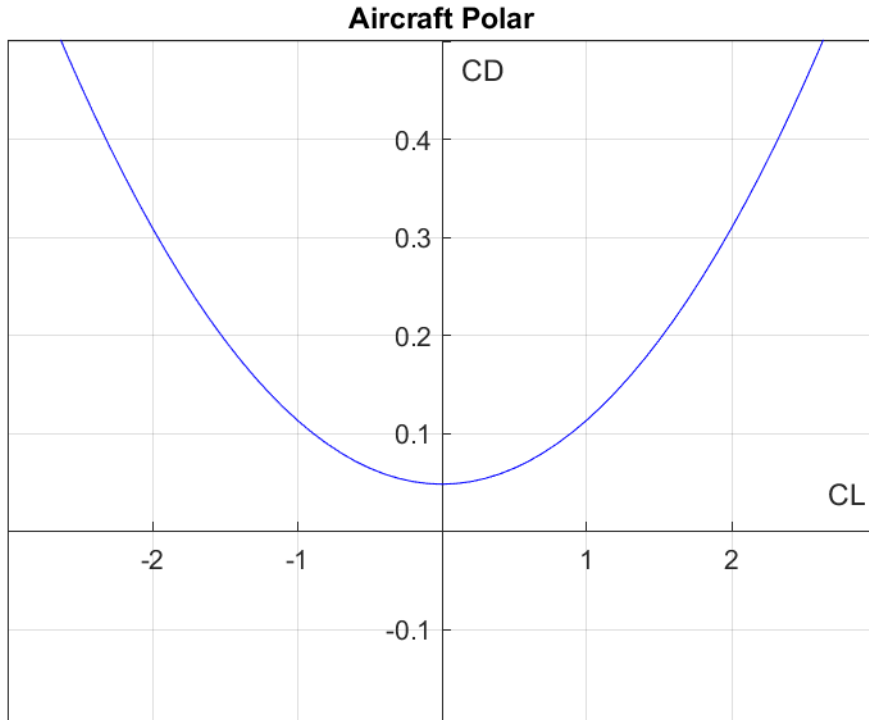


Figure 10: Drag coefficient versus lift coefficient.

As it is shown in Fig 11 the typical value of CD_0 for small general aviation with fixed



landing gear aircraft is between 0.025-0.04. The estimation obtained for Voltic is 0.0483, which is closer to 0.05. It is not between the range proposed by Sadraey, but as it is close, it can be concluded that the result is reasonable. Furthermore, looking at equation 11 it can be noticed that high power and efficiency values, which are common values in aerobatic planes, increase the value of the zero drag estimation.

No.	Aircraft type	C_{D_0}
1	Jet transport	0.015–0.02
2	Turboprop transport	0.018–0.024
3	Twin-engine piston prop	0.022–0.028
4	Small GA with retractable landing gear	0.02–0.03
5	Small GA with fixed landing gear	0.025–0.04
6	Agricultural	0.04–0.07
7	Sailplane/glider	0.012–0.015
8	Supersonic fighter	0.018–0.035
9	Home-built	0.025–0.04
10	Microlight	0.02–0.035

Figure 11: Typical values of CD_0 for different types of aircraft.[1]

7 Maneuver and gust diagram

The maneuver and gust diagrams define the different velocities that aircraft can fly in each situation. The flight envelope is the region where an aircraft can operate safely, and for an aerobatic aircraft, this is essential. The aircraft will be flying most of the time at the limit when performing the different maneuvers, so it is important to know exactly what the limit is so as not to exceed it.

7.1 Maneuver diagram

The maneuver diagram, Figure 12, shows the load factor of the plane for each velocity. This means that the graph is a way to define the maximum and minimum values of the load factor that the aircraft structure should resist.

Usually, the value of the minimum positive load factor is set with the regulation CS-23 [23] because it is an aerobatic aircraft. However, in this case, the load factor is a requirement, so it is set by design. The value of each one is $n_{max} = 8$ and $n_{min} = -5$, which both are greater than the minimum set by the regulation.

On the other hand, the velocities used to develop the diagram have to be computed, and the formulas used to do these calculations are also defined in the CS-23 regulation.

The data used to build the diagram is the following:

- ◊ $V_c = 85 \text{ m/s}$
- ◊ $V_d = 129 \text{ m/s}$
- ◊ $V_a = 84 \text{ m/s}$
- ◊ $V_s = 30 \text{ m/s}$
- ◊ $V_f = 45 \text{ m/s}$

The procedure followed to compute all these velocities is explained in appendix B.

As for all the lift coefficients, it has been chosen the ones from similar aircraft or using Mohammad H Sadraey's book [1], like it has been seen in section 5.

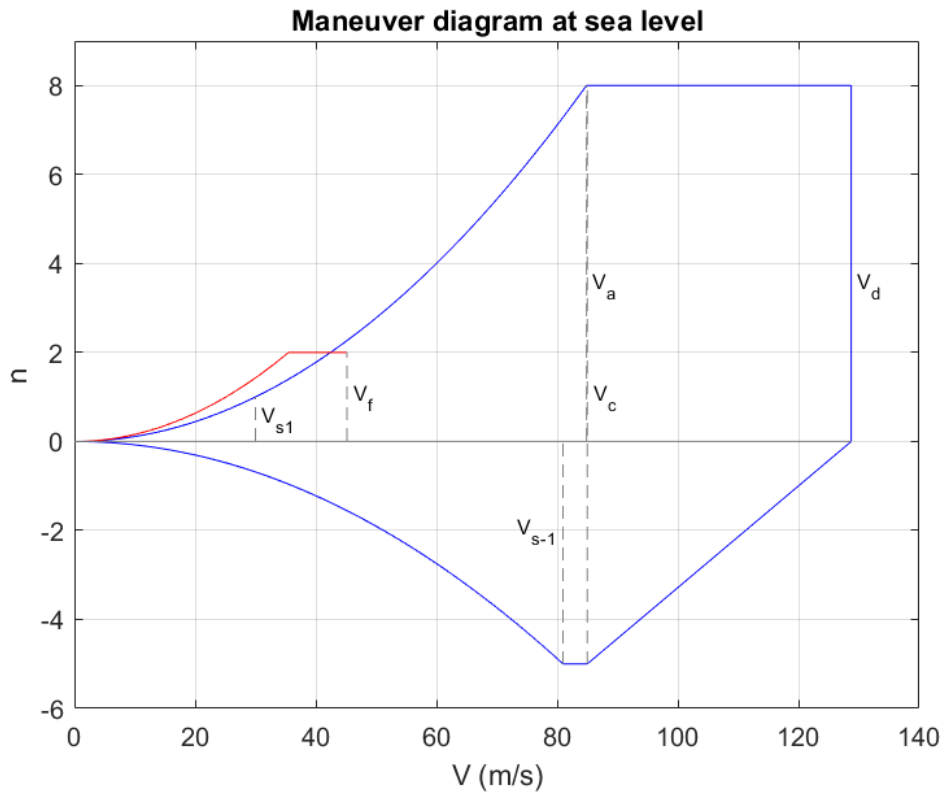


Figure 12: Flight maneuver envelope at sea level.

As can be seen in Figure 12, the results shown seem correct because the aircraft achieves the maximum load range from the cruise speed to the maximum speed. From V_c , the positive load factor is constant, which is perfect, but the negative starts to decrease. It is not a problem because the maneuvers are usually done in the positive load factor range, not in the negative.

7.2 Gust diagram

The gust diagram works the same way that the maneuver one, but takes into account the possible gusts during the flight.

The extra speed due to the gusts is defined by the prevalent regulation, which sets the values as shown below:

- ◊ $V_{c_{gust}} = 15.24 \text{ m/s}$
- ◊ $V_{d_{gust}} = 7.62 \text{ m/s}$
- ◊ $V_{b_{gust}} = 20.11 \text{ m/s}$

With all of this information, the gust diagram can be built.

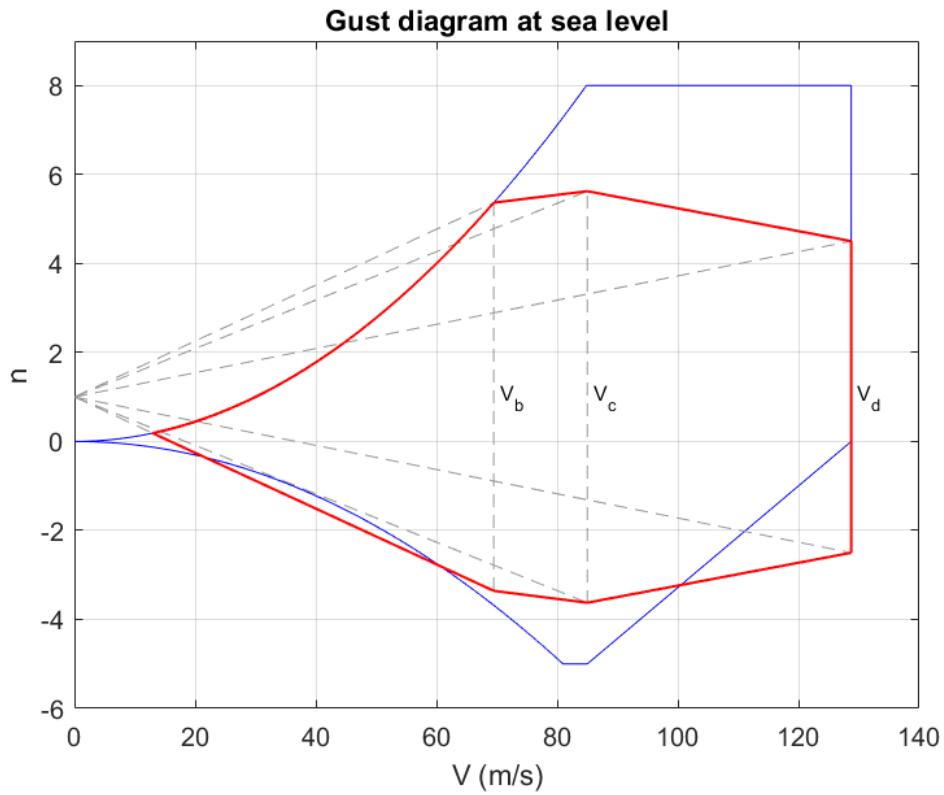


Figure 13: Flight gust maneuver envelope at sea level, highlighted in red.

As can be seen in the figure above, the design speed for maximum gust intensity (V_b) can be determined. The velocity is found where the maneuver diagram and the line plotted with $V_{b_{gust}}$ intersect. Hence, the value is:

$$V_b = 69 \text{ m/s}$$

Also, Figure 13 shows that the gust diagram is much smaller than expected. A small flight envelope is a problem because, in windy conditions, the plane could not fly at maximum performance, but it would have to fly at 5.5 g maximum.

The main reason for the problem is that all the calculations have been made using CS-23 standards, which are conservative. In fact, the regulation has to be conservative because it affects a wide range of similar aircraft, however, each of these airplanes conducts very differently.

Therefore, the principal characteristic of an aerobatic plane is that it can support high gs, and probably, the regulation is not so well prepared for this case. So, a way to find another more accurate flight envelope could be doing flight tests like many other companies.



8 Electric propulsion

Since the early start of this project, one of the targets was to be environmentally friendly, which is why electric propulsion has been chosen. In this section, we are going to study some of the most important parameters to set up our propulsion system.

The propulsion system is composed mainly by:

- ◊ **Battery:** Electricity generator
- ◊ **Electronic Speed Controller (ESC):** Controls and regulates engine speed.
- ◊ **Electric motor:** Convert electricity to mechanic energy.
- ◊ **Propeller:** Convert mechanic energy to thrust.

8.1 Propeller

In order to size the propeller, PropCalc[24] has been used. This software computes the performance data of propellers with a given geometry, notably in-flight thrust and power drain across the utilizable airspeed range. By comparing different propellers given by the program, **Carrera Primus (alt) 15" x 13"** propeller with **E392** airfoil has been selected due to its performance in high velocities. As it can be seen in Figure 14, it has been decided to use a propeller with variable pitch, 3 blades, and a diameter of 2.03 m. The number of blades and the diameter has been set by looking at propellers used in reference aircraft.

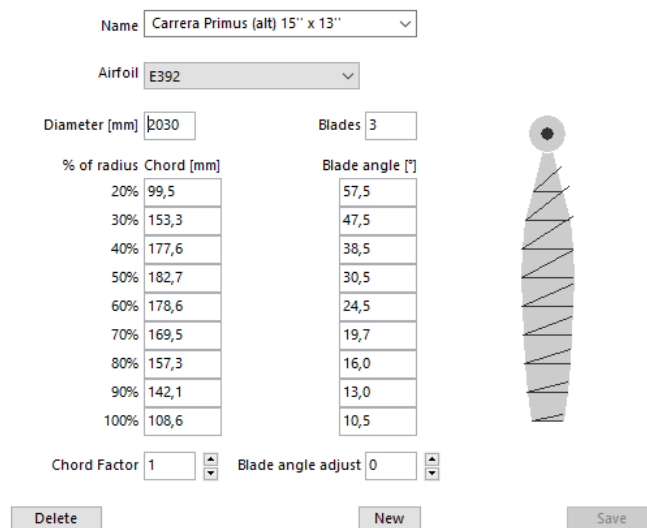


Figure 14: Blade parameters. Software from [24].



The cruise velocity selected for Voltic was $V_c = 85$ m/s. Therefore the optimum rpm for the best propeller-transmission efficiency is **3000 rpm**.

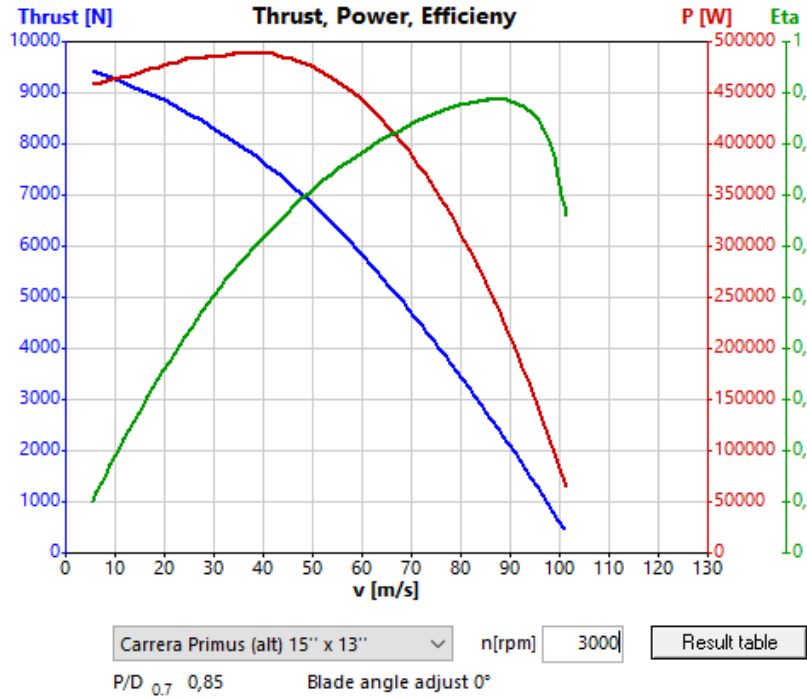


Figure 15: Thrust, power and propeller efficiency vs velocity. Software from [24].

The required thrust to fly at constant cruise speed without climb can be calculated as:

$$T = D ; L = W$$

$$T = (C_{D_o} + kC_L^2) \cdot \frac{1}{2} \rho v_\infty^2 S = (C_{D_o} + k(\frac{2W}{\rho v_\infty^2 S})^2) \cdot \frac{1}{2} \rho v_\infty^2 S \quad (14)$$

Where the drag polar has been calculated in section 6.

Thrust and power can be expressed without dimensions as.

$$C_T = \frac{T}{\rho D^2 (n_H D)^2} \quad (15)$$

$$C_P = \frac{P_H}{\rho D^2 (n_H D)^3} \quad (16)$$

It has been proved that these coefficients can be expressed as third degree polynomials which adjust pretty well to experimental data.



$$C_T = C_{T_0} + C_{T_1} \cdot J + C_{T_2} \cdot J^2 + C_{T_3} \cdot J^3 \quad (17)$$

$$C_P = C_{P_0} + C_{P_1} \cdot J + C_{P_2} \cdot J^2 + C_{P_3} \cdot J^3 \quad (18)$$

Where $J = \frac{v_\infty}{n_H D}$ is the advanced ratio. By taking 4 points from Figure 15 and solving the next system, thrust coefficients ($C_{T_0} \ C_{T_1} \ C_{T_2} \ C_{T_3}$) are obtained. And the same can be done for power coefficients.

$$\begin{pmatrix} C_{T_{(1)}} \\ C_{T_{(2)}} \\ C_{T_{(3)}} \\ C_{T_{(4)}} \end{pmatrix} = \begin{pmatrix} C_{T_0} & C_{T_1} & C_{T_2} & C_{T_3} \end{pmatrix} \cdot \begin{pmatrix} J_{(1)}^0 & J_{(2)}^0 & J_{(3)}^0 & J_{(4)}^0 \\ J_{(1)}^1 & J_{(2)}^1 & J_{(3)}^1 & J_{(4)}^1 \\ J_{(1)}^2 & J_{(2)}^2 & J_{(3)}^2 & J_{(4)}^2 \\ J_{(1)}^3 & J_{(2)}^3 & J_{(3)}^3 & J_{(4)}^3 \end{pmatrix}$$

Once these coefficients are known, the thrust required for cruise velocity in equation 14 it has been found that the propeller has to spin at $n_H = 47 \text{ rev/s} = 2820 \text{ rpm}$ to which corresponds to a propeller efficiency of:

$$\eta_H = \frac{T \cdot V_c}{P_H} = 0.88 \quad (19)$$

8.2 Motor and battery

To size the battery, the voltage and current consumed by the motor are needed first. These parameters, have been obtained following the procedure explained in section A6.1 from [25].

$$i = Q_m \cdot Kv + i_0 \quad (20)$$

$$V = Q_m \cdot R_{int} \cdot Kv + \omega_m + i_0 \cdot R_{int} \quad (21)$$

Kv , i_0 and R_{int} are the speed constant, zero torque current and internal battery resistance respectively, which are provided by the engine manufacturer. As it was mentioned before, it is going to use Rolls-Royce's power plant, which uses the engine YASA 750 R.

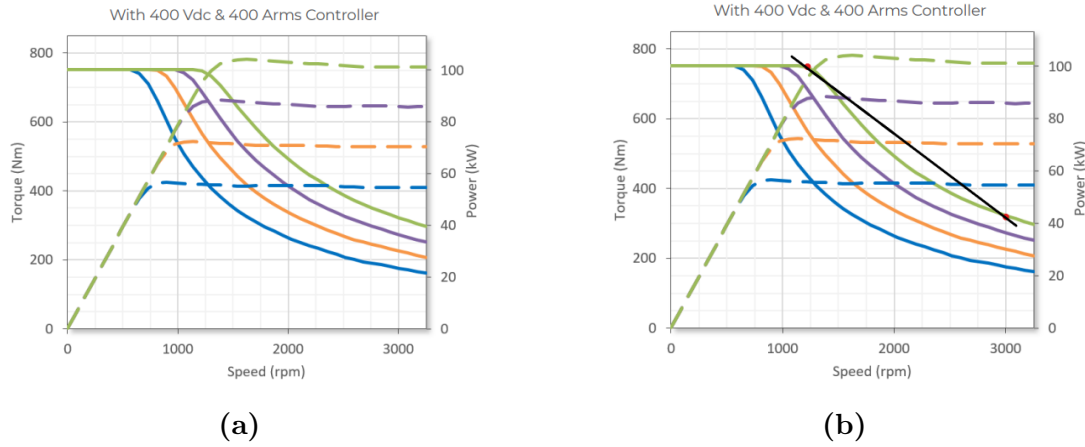


Figure 16: Torque vs rpm for motor YASA 750 R. [26]

From Figure 16a a linear approximation, Figure 16b can be done in order to obtain the relationship between the torque given from the motor and its revolutions per minute, this value is the speed constant.

$$Torque = \frac{300 - 750}{3000 - 1200} \cdot speed + 1050$$

$$|Kv| = 0.25 \text{ Nm/min.}$$

The internal resistance and the zero torque current are not provided by YASA Limited, so based in other similar motors the next values have been assumed.

$$R_{int} = 10 \Omega \quad i_0 = 6 \text{ mA}$$

On the other hand, Q_H is the resistant torque of the propeller and Q_m is the resistant torque needed for the motor in order to spin the propeller. Q_H can be calculated by dividing the propeller power obtained from equation 18 at $n_H = 47 \text{ rev/s}$ over $\omega_H = 2\pi n_H$.

$$Q_H = \frac{P_H}{\omega_H} \quad (22)$$

It should be noted that the motor YASA 750 R, selected for the plane, has a speed range of 0-3250 rpm so it has been decided to use a transmission ratio of $r = 1$ in order to avoid unnecessary losses. Thus, the following assumption has been made $Q_m \cdot W_m = Q_H \cdot W_H$.



Finally, the motor efficiency will be the quotient between the power given to the shaft and the power absorbed from the battery.

$$\eta_m = \frac{Q_m \cdot \omega_m}{V \cdot I} = 0.77 \quad (23)$$

To conclude, it can be said that the propeller-motor transmissions system is pretty well-matched as for the revolutions $n_H = 2820 \text{ rpm}$ needed to fly at stationary flight with cruise velocity the propeller and motor efficiencies are $\eta_H = 0.88$, $\eta_m = 0.77$ respectively.

8.3 Flight time and range

The purpose of this section is to compute the flight time and the range of the aircraft taking into account all the parameters described before. All these parameters are going to be calculated just to verify that the aircraft reaches our *TLR*. The aim of the aircraft it is not to have a great flight time or a wide range. Nevertheless, could be of interest to know this information for some specific flight plans.

It has been chosen an LCO (Lithium Cobalt) battery, which has about 250 Wh/kg energy density. In addition, the calculus showed that 396 kg battery was too much mass, so it has been changed to 300 kg, which is enough to reach the *TLR*. It has an efficiency of 95% and can operate between -20°C and 55°C .

There are many factors of the engine that affect the flight time and the range, all of those have been set in previous sections. The flight time can be calculated as:

$$t = \frac{E_{battery}}{P} = \frac{E_{battery}}{V \cdot I} \quad (24)$$

Where $E_{battery}$ is the product of the battery mass with the energetic density of the battery. In addition, it has been considered that the battery will not be discharged more than 20% of its capacity in order to extend the battery life.

Figure 17 shows the time flight calculated for a specific range of V_{Cruise} , in particular from V_{Stall} to $V_{Cruise} + 10$.

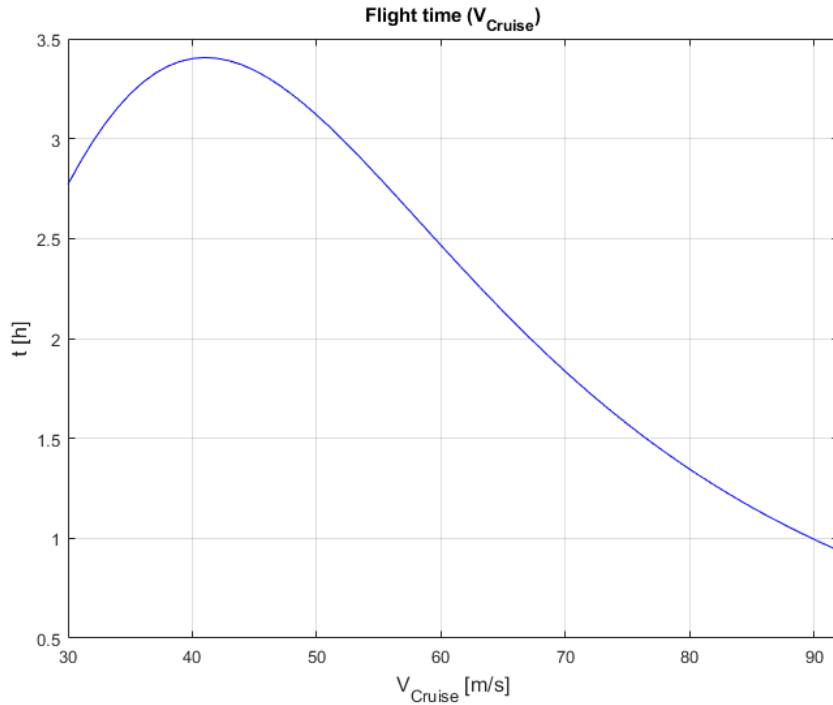


Figure 17: Flight time for 300 kg battery and 250 Wh/h energetic density.

It can be seen that $V_{Cruise} = 42 \text{ m/s}$ is where the propulsive system provides the most flight time, 3.4 h . As the aim of this design, it is not to achieve the maximum flight time, the only parameter that we have to check is if the V_{Cruise} set in the performance's diagram accomplishes our *TLR*. With a battery mass further below the estimated, we achieve the *TLR*.

To compute the range of the aircraft it should be used the following formula 25.

$$R = t \cdot V_{Cruise} \quad (25)$$

Plotting range against the same V_{cruise} range, it is obtained Figure 18

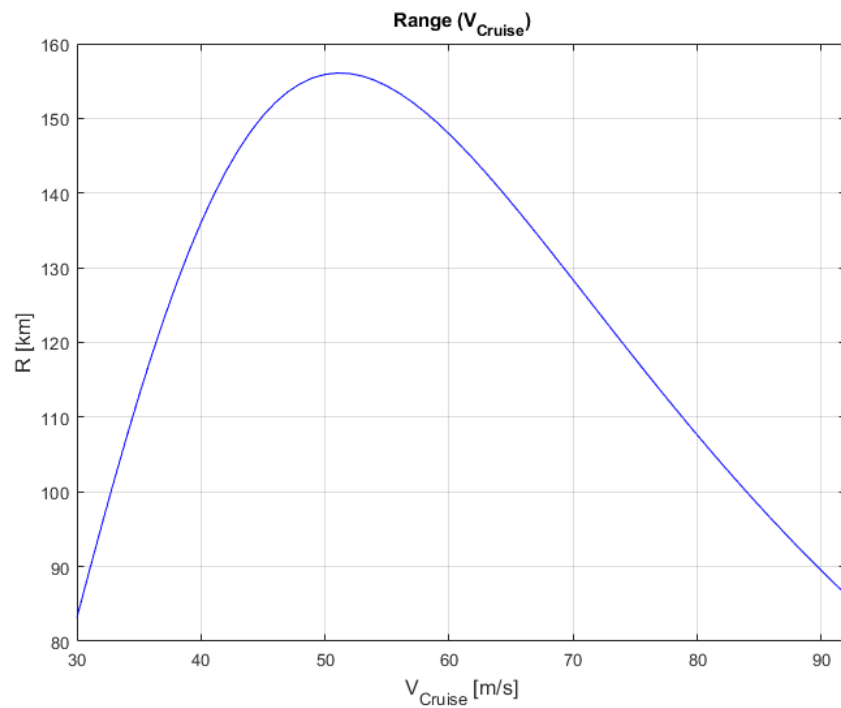


Figure 18: Range for 300 kg battery and 250 Wh/h energetic density.

This plot shows that in order to reach the maximum range, 156 *km*, it has to be set $V_{Cruise} = 51 \text{ m/s}$. However, as we saw before, as the aim of the design is not to achieve the maximum range, it has to be checked if the V_{Cruise} set in the performance's diagram accomplishes our *TLR*, in this case as it has not been set any range *TLR*, range plot is not as important as the flight time plot, however, it can be very useful to know which range Voltic has depended on the V_{Cruise} .



9 Range vs payload

The relationship between the proportion of payload and range on a plane depends among others factors on fuel consumption. As the plane will be electric, the MTOM will remain constant throughout the flight.

9.1 Deduction of range vs payload

As the plane will have a constant payload of one or two people, the variation of the range will not differ much from the other. For a first approximation it will be considered that if there is only one pilot flying, the remaining payload is going to be fulfilled with extra weight (cameras, 0g experiments telemetry instruments, or additional batteries) in order to achieve the 200 kg of payload. For the calculations of range it is used:

$$R = t \cdot V_{Cruise} \quad (26)$$

In the case of battery-powered aircraft, the flight time is equivalent to the time it takes for the battery to discharge, which under ideal conditions is given as:

$$R = t \cdot V_{Cruise} \quad (27)$$

Inserting the flight time into the range equation:

$$R = v_{cruise} \frac{m_{bat} \cdot E}{P_{bat}} \quad (28)$$

The power obtained from the battery is related to the propulsive power required by the aircraft.

$$P_{bat} = \frac{P_{plane}}{\eta_{total}} \quad (29)$$

Where the required power is linked to the weight, the L/D ratio and the flight speed.

$$P_{plane} = D_{plane} v_{cruise} \frac{mg}{L/D} v_{cruise} \quad (30)$$

From the equation 30, the battery power is given as:

$$P_{bat} = \frac{mg}{L/D \cdot \eta_{tot}} v_{cruise} \quad (31)$$

This can be replaced into the range's equation, equation 28.

$$R = v_{cruise} \frac{m_{bat} \cdot E}{\frac{mg}{L/D \cdot \eta_{tot}} v_{cruise}} \quad (32)$$

Finally, the simplified equation is:

$$R = E \cdot \eta_{tot} \frac{1}{g} \frac{L}{D} \frac{m_{bat}}{m} \quad (33)$$

The equation 33 shows the importance of four design factors that determine the range of the aircraft. The first one is the energy density of the battery, which in the past section was fixed at $250Wh/kg$. The second one is the efficiency of the total system, including the battery 0.95, motor 0.77 and propeller 0.88. The result is a total efficiency of 0.64. The lift-drag relation, in this case, is fixed because it was set to a V_{Cruise} of 52 m/s.

9.2 Calculation of range vs payload

Considering 200 kg of payload, which means the totality of the payload, results in 156 km. In contrast, considering only one pilot, which means nearly half of the payload, results in 172 km of range.

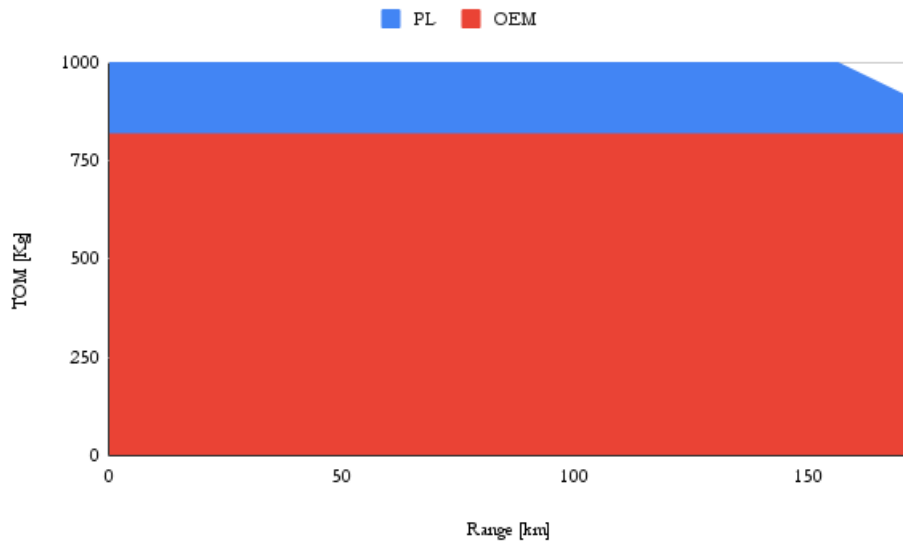


Figure 19: Range vs Payload.

As shown in Figure 19 it is clear that for Voltic, payload it is not as restrictive as other parameters.



10 Wing Design

The wing is one of the most important components of a plane, as it provides the necessary lift force to fly. In this section, a preliminary design will be carried out. The methodology used is based mainly on chapter 5 of Sadraey's book [1].

During the wing design process, 18 parameters must be determined. They are as follows:

1. Wing reference area S_w .
2. Number of wings.
3. Vertical position.
4. Horizontal position.
5. Airfoil.
6. Aspect ratio AR .
7. Taper ratio λ .
8. Tip chord C_t .
9. Root chord C_r .
10. Mean aerodynamic chord.
11. Span b .
12. Twist angle α_t .
13. Sweep angle Λ .
14. Dihedral angle Γ .
15. Incidence i_w .
16. High-lifting devices.
17. Aileron.
18. Other wing accessories.

Parameters 1 and 6 have been set before. Thus, 11 is also fixed. For parameter 2, it has been proven that nowadays, with the advances in aerospace materials such as light aluminum or composites that can handle longer wing spans, a single wing is almost the only practical option in conventional modern aircraft.

For parameter 3, it has been decided to use a **low wing** configuration mainly due to control reasons. With a low wing, the aircraft has higher lateral control, the wing has less down-wash on the tail so it is more effective and can be lighter and is lighter compared with a high-wing structure among other reasons.

Parameter 14 has been set to $\Gamma = 0^\circ$. The primary reason for applying a wing dihedral is to improve the lateral stability of the aircraft. In aerobatic planes high lateral stability could become a maneuverability issue.

Parameter 15, is the angle between the fuselage center line and the wing chord line at its root. As it will be needed to vary constantly during flight, there is no need to determine the wing setting angle for the purpose of aircraft manufacture.

Parameters 4, 16 and 17 are going to be studied in section 12 and 5, 7, 8, 9, 10, 12, 13 and 15 will be discussed next in more detail.



10.1 Airfoil Selection

The airfoil selection is normally made taking into account the cruise conditions of the vehicle. Unlike other typical planes that have very straight and well-defined maneuvers, aerobatic planes are meant to be versatile and have a wide range of movements. As it will be appreciated later, this characteristic ends up sacrificing some of the wing's efficiency.

The ideal airfoil lift coefficient for cruise conditions can be calculated as:

$$Cl_i = \frac{2 \cdot W_{avg}}{\rho V_c^2 S} \cdot \frac{1}{m \cdot n} = 0.39$$

Where $m = 0.95$ and $n = 0.9$, m is a correction factor for the fuselage and other elements contribution to the lift and n adjusts the possible introduction of sweep angle or taper ratio to the wing and also adjusts the lift loss from a 2D airfoil to a 3D wing.

The maximum gross lift coefficient for cruise conditions can be calculated as:

$$Cl_{max_gross} = \frac{2 \cdot W_{MTOW}}{\rho_o V_s^2 S} \cdot \frac{1}{m \cdot n}$$

For this section, it has been assumed a preliminary value of 0.4 for the lift contribution of high lift devices.

$$Cl_{max} = Cl_{max_gross} - Cl_{HLD} = 1.64$$

With this values, at Fig 21 the following airfoils are recommended NACA 63₁ – 412, 64₁ – 412, 65₁ – 412, 65₂ – 415, 64A41.

But as said before, the main goal is to have a wide range of maneuverability and those airfoils are cambered. Cambered airfoils produce a pitch down torque which increases with speed, and this would interfere with the goal of neutral pitch stability. Neutral pitch stability eliminates any pitch response related to airspeed, which at the same time allows for clean straight lines during dives or climbs without requiring elevator adjustment for speed. Hence, a symmetrical airfoil is going to be used.

The best airfoil is the airfoil whose C_m is the lowest, C_d is the lowest, α_s is the highest, $(Cl/Cd)_{max}$ is the highest, and stall quality is docile. The 6-series NACA airfoils were designed to maintain laminar flow over a large part of the chord, thus they maintain a lower C_d compared with four- and five-digit airfoils. In table 7, a comparison between 6-series NACA airfoils with $Cl_{max} \approx 1.64$ is made.



NACA	Cd* _{min}	Cm _o	Cl _α	α _{stall}	Cl _{stall}	(Cl/Cd)max	(t/c)max %
64 ₂ – 015	0.00627	0	0.112	15	1.45	231.6	15
63 ₁ – 012	0.0054	0	0.116	14	1.45	268.52	12
64 ₃ – 018	0.00733	0.004	0.111	17	1.5	204.64	18
66 ₁ – 012	0.00562	0	0.106	14	1.25	222.42	12
63 – 009	0.0049	0	0.111	11	1.15	234.69	9

Table 7: Airfoil characteristic. [27][28]

(*) To estimate the airfoil minimum drag, it has been used the data provided by airfoil tools [27] at a Reynolds number of $Re = \frac{V_c \rho S L c}{\mu} = \frac{82 \cdot 1.225 \cdot 1.36}{1.813 \cdot 10^{-5}} = 7 \cdot 10^6$. The cord has been calculated assuming a rectangular wing, this will not be the final configuration but it is acceptable to proceed with the airfoil comparison.

If the wing is designed for a high subsonic passenger aircraft, it is desirable to select the thinnest airfoil (the lowest (t/c)max). The reason is to reduce the critical Mach number.

Criteria	Weight	64 ₂ – 015		63 ₁ – 012		64 ₃ – 018		66 ₁ – 012		63 – 009	
		g	p	gxp	p	gxp	p	gxp	p	gxp	p
(Cl/Cd) _{max}	5	2.69	13.45	5	25	1	5	2.11	7.11	2.88	14.4
Cl _α	4	1.4	5.6	5	20	1.33	5.32	1	4	1.33	5.32
α _{stall}	3	3.67	11.01	3	9	5	15	3	9	1	3
Cm _o	2	5	10	5	10	1	2	5	10	5	10
(t/c)max %	4	2.34	9.36	3.67	14.68	1	4	3.67	14.68	5	20
SUM	18		49.42		78.68		31.32		14.78		52.72
OWA			0.55		0.87		0.35		0.16		0.56

Table 8: Ordered Weight Average calculations to select the airfoil.

Therefore, the best airfoil according to the OWA method is the **NACA 63₁ – 012**.

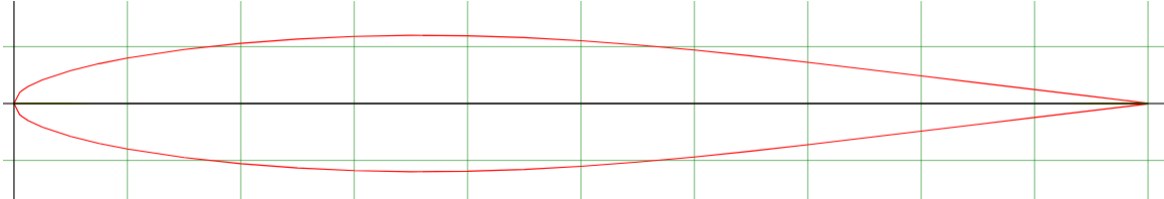


Figure 20: NACA 63₁ – 012. [27]

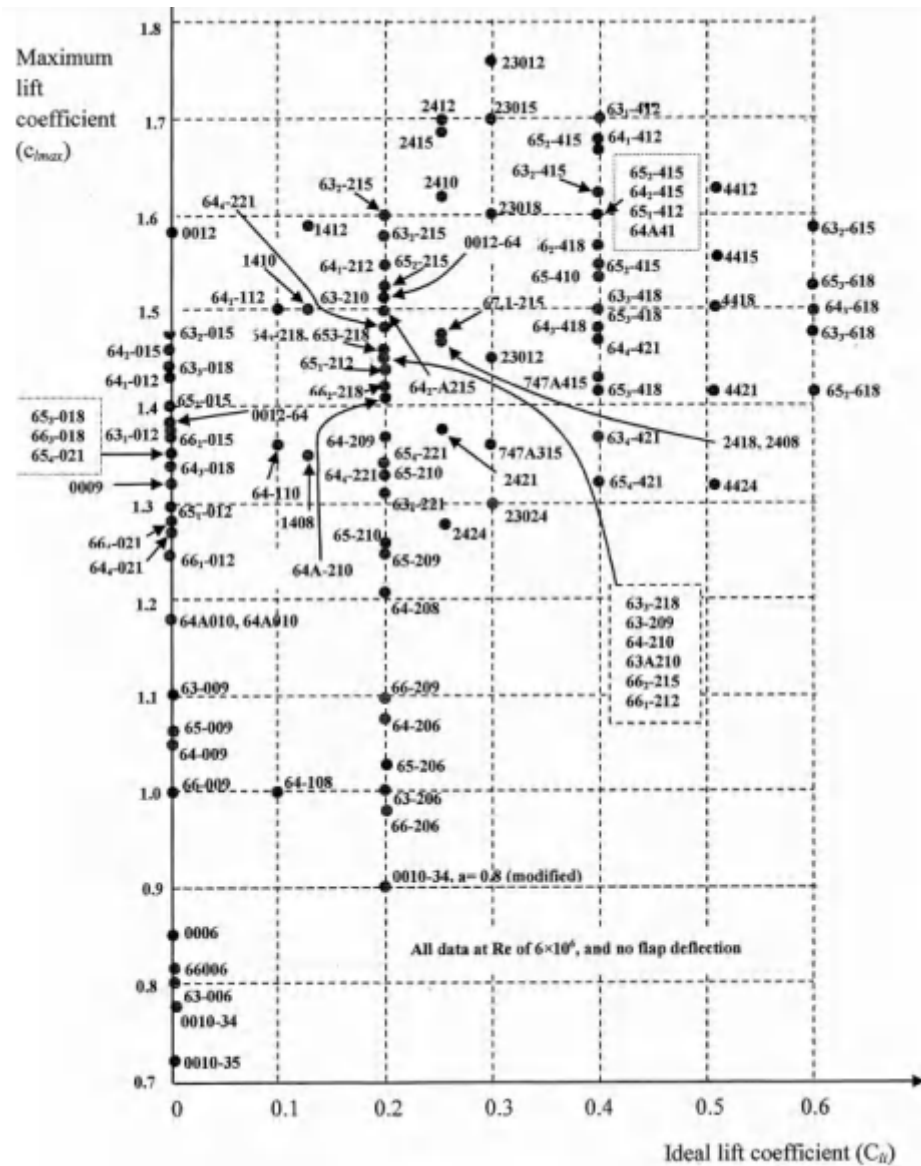


Figure 21: Maximum lift coefficient versus ideal lift coefficient for several NACA airfoils.[1]

10.2 Sweep angle

“Wing sweep is primarily used on aircraft that fly in the transonic and supersonic regions. The sweep has the effect of delaying the formation of shock waves on the surface of the wing caused by the compressibility of air at high speeds”[29]. As the aircraft is not intended to fly at either transonic or supersonic velocities, the sweep angle will be set to zero. $\Lambda = 0^\circ$.

10.3 Taper ratio & Twist angle

The taper ratio λ is defined as the ratio between the tip chord C_t and the root chord C_r .

$$\lambda = \frac{C_t}{C_r}$$

A wing with a rectangular planform has a larger downwash angle at the tip than at the root. Therefore, the effective angle of attack at the tip is reduced compared with that at the root. Thus, the wing tip will tend to stall later than the root.

A rectangular wing planform is structurally inefficient since there is a lot of area outboard, which supports very little lift. Wing taper will help resolve this problem. The first estimate of the taper ratio will be determined by lift distribution calculations.

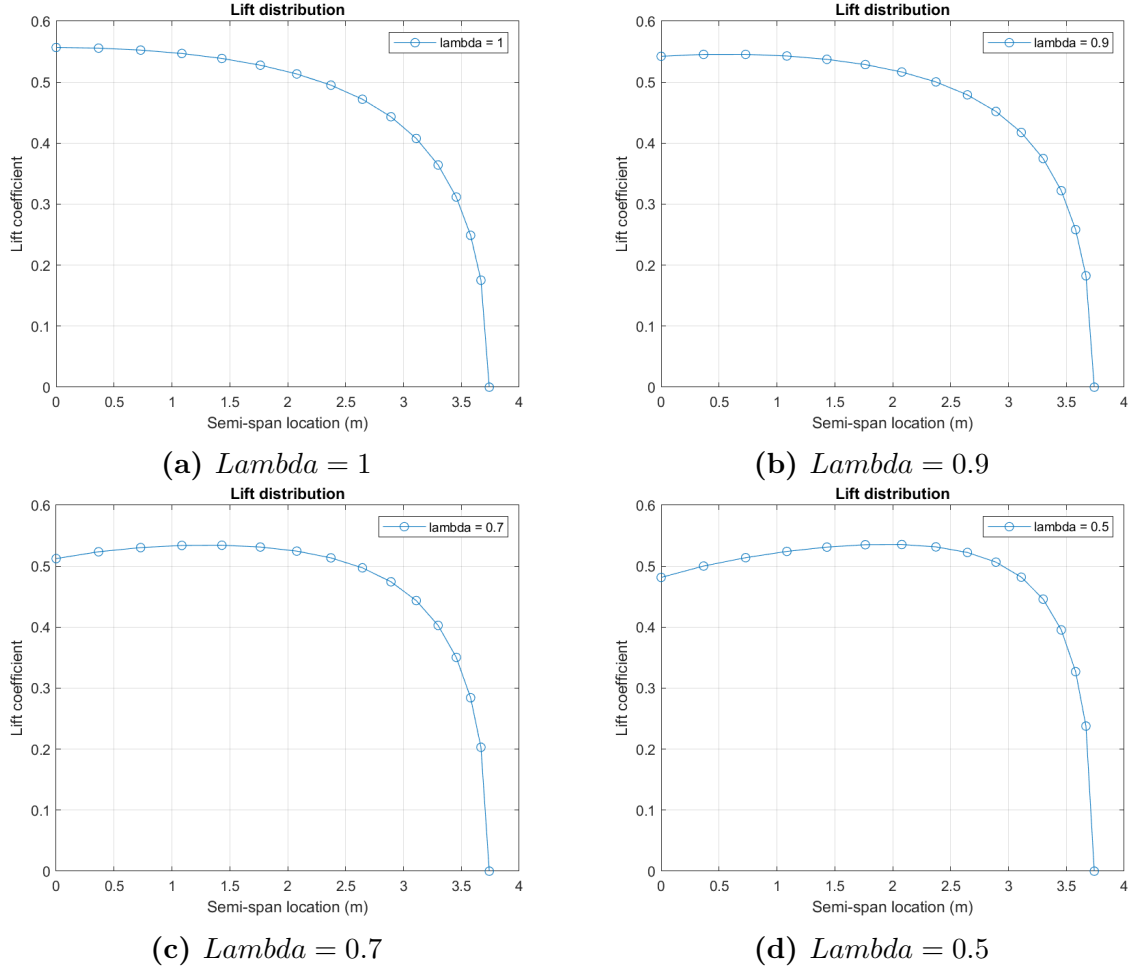


Figure 22: Lift distributions for different taper ratios. Code extracted from [1].



And the respective wing lift coefficient for each taper ratio is:

$$CL_{wing}^{(a)} = 0.4828 \quad CL_{wing}^{(b)} = 0.4854 \quad CL_{wing}^{(c)} = 0.4877 \quad CL_{wing}^{(d)} = 0.4832$$

As can be observed, even though the differences are slight. The best taper ratio is $\lambda = 0.7$.

These lift distributions have been calculated assuming a geometric wing twist $\alpha_t = 0^\circ$. Later on, different geometric twist angles have been tested. By increasing the geometric twist angle, the lift coefficient increased at the tips. Nevertheless, having a geometric twist angle in aerobatic maneuvers could be counterproductive by increasing excessively the bending moments. As none of the reference aircraft of this project have a geometric twist, the geometric twist angle will be discarded and an aerodynamic twist angle could be studied in further iterations of the wing design process.

Is the wing lift coefficient enough?

To verify an acceptable wing design. The wing should, at least, provide enough force at cruise speed to overcome the weight.

$$L = MTOW = 1000\text{kg} \quad L = \frac{1}{2}\rho SV_c^2 CL_{wing}$$

$$L = \left(\frac{1}{2} \cdot 0.863 \cdot 10.18 \cdot 82^2 \cdot 0.4877\right)/9.81 \approx 1470\text{kg} > MTOW$$

To take off the speed needed is 57 m/s or 205 km/h:

$$L = \left(\frac{1}{2} \cdot 1.225 \cdot 57^2 \cdot S \cdot 0.4877\right)/9.81$$

To reduce this speed, or to take off earlier high lifting devices such as flaps are used. One top requirement was to take off before 200 m. In this way, the acceleration, time, and thrust required without flaps are:

$$\sum F_x = m \cdot a_x$$

$$\sum F_y = m \cdot a_y$$

$$T - D - F_f^{(*)} = m \cdot a_x$$

$$L + N - W = 0$$

$$\begin{cases} L = \frac{1}{2}\rho_{SL}v^2sCL_{wing} \\ D = \frac{1}{2}\rho_{SL}v^2s(CD_o + kCL_{wing}^2) \\ v_f = v_o + a_xt \\ x_f = x_o + v_ot + \frac{1}{2}a_xt^2 \end{cases} \quad \frac{1}{2}\rho_{SL}v^2sCL_{wing} + \cancel{N} - W = 0 \rightarrow$$



$$t = \sqrt{\frac{2W}{\rho SCL_w a_x^2}} \rightarrow x_f = x_0 + v_o t^0 + \frac{1}{2} a_x (\sqrt{\frac{2W}{\rho SCL_w a_x^2}})^2 \rightarrow a_x = \frac{W}{\rho SCL_w x_f} = 8 \text{ m/s}^2$$

$$t = 7s$$

$$T = ma_x + \frac{1}{2}\rho(a_x t)^2 S(CD_o + kCL_w^2) = 9.25 \text{kN}$$

(*) Friction forces have been neglected due to their minimal contribution, and at this stage of the design process the accuracy of several estimated parameters is not high, the friction force is not relevant.

To achieve this thrust, the motor should spin at **3500** rpm which is 250 rpm more than the maximum rotational speed recommended by the manufacturers[26] of the motor.



Figure 23: Revolutions required to reach take-off thrust.[24]

As the parameters of take-off velocity, acceleration, time, and thrust obtained before are quite acceptable to meet the top level requirement of taking off at 200 m. It has been decided not to use high lifting devices. As in previous sections has been proved that autonomy is more than enough. Battery weight will be sacrificed to put a gearbox to reach 3500 rpm.



10.4 Final wing configuration

This way, the main final wing parameters can be found in table 9.

Airfoil	S_w [m ²]	b[m]	C _r [m]	C _t [m]	α_t [°]	Λ [°]	Γ [°]	i_w [°]
NACA 63 ₁ – 012	10.18	7.48	1.58	1.1	0	0	0	0

Table 9: Final wing configuration parameters.

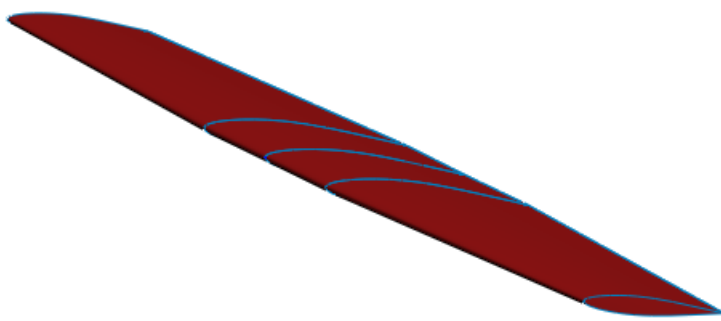


Figure 24: Final wing configuration CAD.



11 Tail design

The tail of an airplane is the part that gives it stability. As it is said in section 3, the type of tail chosen for the design is the conventional tail. The tail consists of two main elements, the horizontal and vertical stabilizer. Both have to be optimally designed to achieve the best performance possible.

11.1 Horizontal stabilizer

The main aspects of the horizontal stabilizer are the airfoil, surface, aspect ratio, and angle of incidence. These four features are going to be computed in this section.

11.1.1 Tail surface

The surface of the tail is important because it is the geometric parameter that determines the lift coefficient that the tail will do. After, it will influence which airfoil to select to put on the airplane. To calculate the surface, first, the optimum distance between the horizontal stabilizer and the aerodynamic center has to be computed.

The calculations to obtain the distance are based on the Sadraey book [1], which is considered for lightweight aircraft with low drag. The objective of this method is to find the maximum value possible for the distance, but at the same time, the minimum value for the horizontal surface. Therefore, to compute it, the wetted area of the aft fuselage is needed.

$$S_{wet_{aft}} = S_{wet_{aft(fus)}} + S_{wet_h} \quad (34)$$

Where $S_{wet_{aft(fus)}}$ is the wetted area between the aerodynamic center and the trailing edge of the fuselage. Assuming it is a pyramid, hence the wetted area is:

$$S_{wet_{aft(fus)}} = L_{aft(fus)} \left(\frac{2h_{fus} + 2a_{fus}}{2} \right) \quad (35)$$

Where h_{fus} is the height of the fuselage and a_{fus} is the width, both determined in section 13. Moreover, it can be assumed that the wetted tail area is twice the surface area. It is also known that the surface area is a function of the tail volume coefficient:

$$S_{wet_h} \approx 2S_h \quad (36)$$

$$S_h = \frac{\bar{c} \bar{S} \bar{V}_H}{l} \quad (37)$$



So:

$$S_{wet_h} \approx 2 \frac{\bar{c} \bar{S} \bar{V}_H}{l} \quad (38)$$

\bar{V}_H is the ratio of the horizontal tail compared to the wing. There is not much information about an aerobatic airplane, so the value is taken from Sadraey [1]. For a GA aircraft with a single prop-driven engine, $\bar{V}_H = 0.7$. Finally, the equation to work with is the following:

$$S_{wet_{aft}} = L_{aft(fus)}(h_{fus} + a_{fus}) + 2 \frac{\bar{c} \bar{S} \bar{V}_H}{l} \quad (39)$$

Like it said before, the objective is to find the minimum tail surface that can stabilize the airplane. Thus, it can be minimized by a derivative and equalized to 0. Also, It is assumed that $L_{aft(fus)} = l$, which is not correct, but for this type of aircraft is close enough.

$$\frac{\partial S_{wet_{aft}}}{\partial l} = (h_{fus} + a_{fus}) - 2 \frac{\bar{c} \bar{S} \bar{V}_H}{l^2} = 0 \quad (40)$$

Working with the equation above, l_{opt} can be obtained:

$$l_{opt} = K_c \sqrt{\frac{2 \bar{c} \bar{S} \bar{V}_H}{h_{fus} + a_{fus}}} \quad (41)$$

Notice that appeared a term that was not in previous calculations. K_c is a correction factor for those aircraft that are not conical. In this case, it is pyramidal, not conical, so it has a value of $K_c = 1.4$. Finally, all the data used is summed up in the following table.

K_c	$S [m^2]$	$\bar{c} [m]$	\bar{V}_H	$h_{fus} [m]$	$a_{fus} [m]$
1.4	10.18	1.35	0.7	1	1.1

Table 10: Horizontal stabilizer parameters.

With all this information, the tail surface can be computed.

$$S_h = \frac{\bar{c} \bar{S} \bar{V}_H}{l} = 2.26 \text{ } m^2$$

11.1.2 Geometric parameters

At this point, the main characteristics of the tail are already calculated, therefore all that is left to determine is the remaining parameters, such as the aspect ratio or the chord.

Firstly, the easiest feature to calculate is the aspect ratio, which is 2/3 of the aspect ratio



of the wing, as says M. H. Sadraey [1].

$$AR_h = \frac{2}{3} AR_w = 3.67 \quad (42)$$

Another important parameter that will contribute to determining the other geometric characteristics is the taper ratio. For this case, no formula can be used with the data known. Thus, the solution is to use related aircraft as a reference.

	Sbach 342	Sukhoi su 29	RR ACCEL	Extra 300L
λ	0.63	0.80	0.62	0.65

Table 11: Horizontal stabilizer taper ratio from reference aircraft.

Doing an arithmetic mean, the taper ratio for the horizontal tail should be 0.68. However, it is close to the taper ratio selected for the wing, which is 0.7. Moreover, a higher taper ratio gives more lift at the tip of the stabilizer, which helps to do a roll movement. So:

$$\lambda = 0.7$$

With this information, the remaining parameters can be computed doing the following equation system given by Sadraey [1].

$$\left. \begin{aligned} AR_h &= \frac{b_h}{\bar{c}} \\ \bar{c} &= 2/3 c_r \frac{(1+\lambda+\lambda^2)}{(1+\lambda)} \\ \bar{c} &= \frac{S_h}{b_h} \end{aligned} \right\} \quad (43)$$

The unknown values of the equations are the tail wingspan (b_h), the mean aerodynamic chord (\bar{c}) and the tail chord at the root (c_r). Solving the system, the values of the variables are:

- ◊ $b_h = 2.88 \text{ m}$
- ◊ $\bar{c} = 0.78 \text{ m}$
- ◊ $c_r = 0.92 \text{ m}$
- ◊ $c_t = 0.64 \text{ m}$

There is another parameter, which is the tail chord at the tip (c_t). It has been calculated with the definition of the taper ratio, defined in section 10.3.



11.1.3 Airfoil selection

The airfoil of the horizontal stabilizer has to generate a good amount of lift while creating the minimum drag and pitching moment possible. Also, it has to have a large lift coefficient slope ($C_{L\alpha}$), to achieve a stall later than the wing.

In addition, the horizontal tail has to be clean of the compressibility effect. To do so, the tail airfoil must be thinner than the wing. In this case, the wing airfoil is a NACA 63₁ – 012 which has a maximum thickness of 12%.

Taking into account all of these conditions, the best airfoil to select is the NACA 0009. Moreover, this is the typical airfoil that is chosen for the GA aircraft, so it is probably the best selection possible.

11.1.4 Incidence angle

The incidence is the angle given to the tail to nullify the pitching moment generated by the wing, usually on cruise flights. However, for an aerobatic aircraft, there is no cruise flight as is regularly understood. Instead, during the flight, the plane will do any type of maneuver.

Therefore, the aircraft has to be able to fly in a normal steady flight or in an inverted one. To achieve this, the horizontal stabilizer has to behave equally for every type of flight, and the only way to accomplish it is by setting the tail to a 0° incidence ($i_h = 0^\circ$).

11.2 Vertical stabilizer

The vertical stabilizer, unlike the horizontal, controls the directional stability. The procedure followed to calculate the different parameters of the stabilizer is similar to the one used for the horizontal stabilizer and is extracted from the Sadraey book [1].

11.2.1 Surface

The surface of the vertical stabilizer is the parameter that determines the lift of the tail on the y axis. Firstly, the equation needed to compute the area is the same as the one used for the horizontal stabilizer:

$$S_v = \frac{\bar{c} \bar{S} V_V}{l} \quad (44)$$

The only change for the horizontal surface is the volume coefficient, which a typical value of this type of aircraft is ($V_V = 0.04$). The parameter l is the distance between the aerodynamic center of the plane and the vertical tail. Usually is calculated as a function of the directional stability. However, in order to do a first approximation, the distance is



assumed to be the same as the calculated for the horizontal tail, in section 11.1.1. Finally, the horizontal tail area is the following.

$$S_v = \frac{\bar{c} \bar{S} \bar{V}_V}{l} = 0.72 \text{ m}^2$$

11.2.2 Geometric parameters

Once the surface is calculated, other parameters can be determined by calculating them or simply approximating them using reference data. These geometric parameters are the sweep angle, the aspect ratio, the taper ratio, the wingspan, and the chord, at the root and the tip.

Firstly, the aspect ratio. Different from the horizontal tail, there is no specific formula that links the aspect ratio of the wing with the aspect ratio of the tail. Instead of that, it has to be approximated, at least for this phase of the design.

Different aspect ratios have different impacts on the final aircraft, and each one has its benefits and flaws. For example, a high aspect ratio vertical tail has more directional control, but it is prone to fatigue and is longitudinally destabilizing.

The key factor to choose between a high or low aspect ratio is that the aircraft has to be as efficient as possible and has to be able to do every maneuver right. Therefore, the aspect ratio selected is 2, which is the maximum value possible within the range of typical values.

$$AR_V = 2$$

The taper ratio, as said in earlier sections, is the relation between the chord at the tip and the root. However, these two parameters are not known, so the taper ratio will be determined using reference aircraft.

	Sbach 342	Sukhoi su 29	RR ACCEL	Extra 300L
λ	0.40	0.41	0.43	0.44

Table 12: Vertical stabilizer taper ratio from reference aircraft.

Given the data, the taper ratio chosen for the vertical stabilizer is set to 0.4.

$$\lambda = 0.4$$

The last parameter that is going to be approximated is the sweep angle, which is defined as the angle between the z axis and the leading edge of the vertical tail. There is no



method to choose the perfect sweep angle for the airplane, instead of doing an iterative process. In this case, to do an iterative process for a conceptual design is exaggerated, so the value chosen is typical for a GA propelled aircraft.

$$\Lambda = 35^\circ$$

The last four values are going to be calculated with an equation system, similar to the procedure followed for the horizontal tail.

$$\left. \begin{array}{l} AR_v = \frac{b_v}{\bar{c}} \\ \bar{c} = 2/3 c_r \frac{(1+\lambda+\lambda^2)}{(1+\lambda)} \\ \bar{c} = \frac{S_v}{b_v} \\ \lambda = \frac{c_t}{c_r} \end{array} \right\} \quad (45)$$

Solving the system, the values of the variables are:

- ◊ $b_v = 1.20 \text{ m}$
- ◊ $\bar{c} = 0.60 \text{ m}$
- ◊ $c_r = 0.81 \text{ m}$
- ◊ $c_t = 0.32 \text{ m}$

Note that all the values calculated above are used as a reference to do the first approach to the design. Later, in the next phases, the values could change to fulfill the needs of the aircraft.

11.2.3 Airfoil selection

The airfoil selected for the vertical tail has to create the lift necessary to maneuver the aircraft.

The main feature of the airfoil is that it has to be symmetrical because it can not generate any yaw moment when flying in a steady flight.

In addition, another requirement is that the vertical tail has to be clean of the compressibility effect. To satisfy that, the thickness of the tail airfoil has to be lower than the wing.

Considering the two factors commented on above, the airfoil selected is the same as the one for the horizontal stabilizer, and it is the NACA 0009.



12 Stability and control

Stability is a measure of how an object tends to behave in the event of a disturbance. If an object tends to recover the initial position it is stable, in addition, the faster it recovers, the more stable it is. In contrast, if an object tends to move away from its initial position, the object is unstable.

In aeronautics, it can be studied the stability studying the dynamics of the aircraft and parameterizing its behavior depending on some parameters. Usually consist of certain coefficients that depend if $Coeff > 0$, $Coeff < 0$ or $Coeff = 0$ the aircraft will behave stably or not.

12.1 Pitching stability

One of the most studied stability fields is pitching stability. It is very important to know the purpose of the aircraft. This will set a range of values where momentum coefficients can be suited in order to achieve the expected behavior.

As it was shown before, the pitching momentum coefficient can be decomposed into different momentum contributions. “Conceptual design of an aerobatic trainer aircraft” [30] report, provides a formula to compute all the aircraft momentum coefficient, equation 46. This formula can be used considering the following hypothesis:

- ◊ Rigid airplane: Any pair of particles always will be at the same distance.
- ◊ Linear aerodynamics (not big angles of attack).

That is to say that the calculation that is going to be done is useful for the cruise phase, whereas the acrobatics phase should be studied using specialized software for studying the airplane's dynamics.

$$C_m = C_{Lw} (\overline{X}_{cg} - \overline{X}_{acw}) + C_{mw} + C_{mfus} + C_{mw\delta_f} \delta_f - \eta_h \frac{S_h}{S_w} C_{Lh} (\overline{X}_{ach} - \overline{X}_{cg}) \quad (46)$$

Where \mathbf{C}_{Lw} is the wing lift coefficient, \overline{X}_{cg} is the fractional length of CG center, \overline{X}_{acw} is the fractional length of wing aerodynamic center, \mathbf{C}_{mw} is the pitching moment contribution of the wing, \mathbf{C}_{mfus} is the pitching moment contribution of the fuselage, $\mathbf{C}_{mw\delta_f}$ is the change in the pitching moment of the wing due to flap deflection, δ_f is the flap deflection angle, η_h is the ratio of the dynamic pressures at the horizontal tail, S_h and S_w are the surface area of the tail and the wing respectively, \mathbf{C}_{Lh} is the lift contribution of the horizontal tail and \overline{X}_{ach} is the fractional length of the aerodynamic center of the horizontal tail.



For this specific case, $\mathbf{C}_{\text{mw}} = 0$ due to the wing's airfoil, $\mathbf{C}_{\text{mfus}} = 0$ as it is not going to be studied and also can be considered zero, $\mathbf{C}_{\text{mw}\delta_f} = 0$ because it has been chosen not to use hyper-supporting devices, flaps, in Voltic's configuration.

Taking all mentioned into account, it is going to be used a method of calculation where it is "set" a desired Cm_α and a desired Cm for cruise and as a result of that, it is going to be fixed the position of the Payload, wing and tail. To be able to compute all these parameters, it is necessary to include the C.G formula for discrete points of mass, equation 47.

$$X_{cg} = \frac{\sum_{n=1}^n m_i X_i}{\sum_{n=1}^n m_i} \quad (47)$$

Using Voltic's data:

$$X_{cg} = \frac{(m_{\text{enginebattery}} \cdot 20\% + PL \cdot \mathbf{x} + m_{\text{wing}} \cdot \mathbf{y} + m_{\text{fus}} \cdot 25\% + m_{\text{tail}} \cdot tail_{pos})}{1000}$$

Where m_i is the mass of the object, i all measurements are dimensionless referenced from the fuselage tip. Note that x and y are the positions that want to be found and $tail_{pos}$ is a result of y considering the information found in section 11, Tail Design. Moreover, the position of C.G from the mass of the engine and batteries was selected using Extra 330LE as a reference, and the C.G position of the fuselage approximated it as a pyramid, that is to say, that the C.G is at his 25% of the total height.

With all this information in mind, it is expected to have negative but nearly zero Cm for the cruise, and a $Cm_\alpha = 0$ in order to make the pilot capable of having the maximum maneuverability without making the aircraft unsteady ($Cm_\alpha > 0$). Figure 25 is the result of plotting the surface of Cm depending on the x and y position and the line of x and y which ensures $Cm_\alpha = 0$.

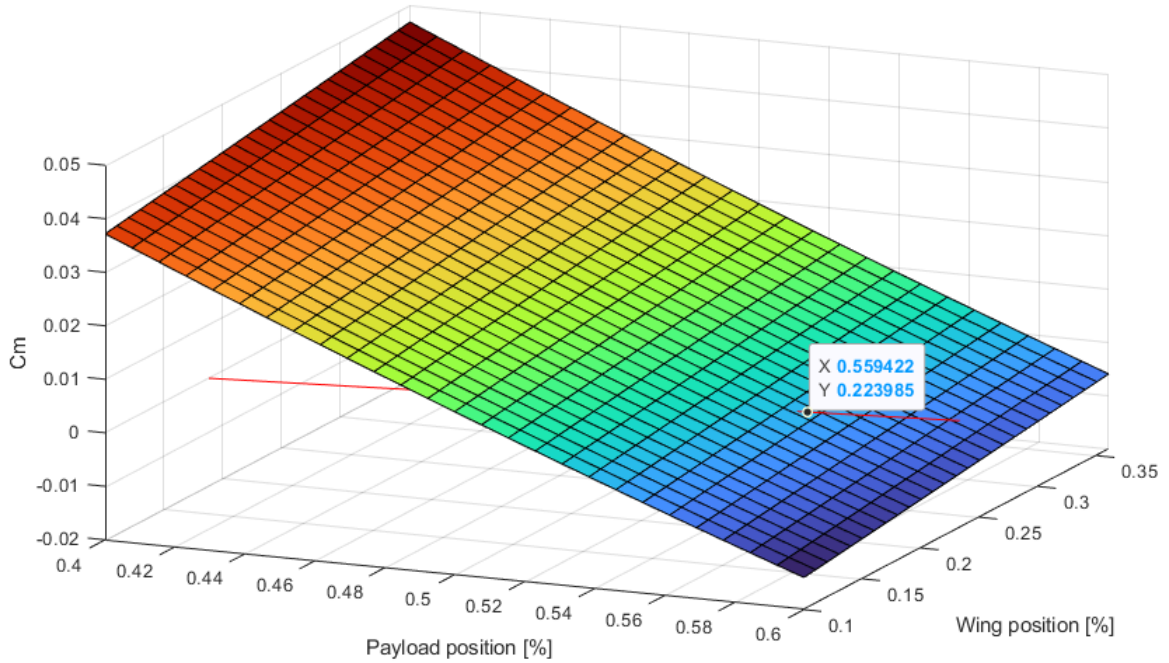


Figure 25: C_m distribution for cruise against x and y .

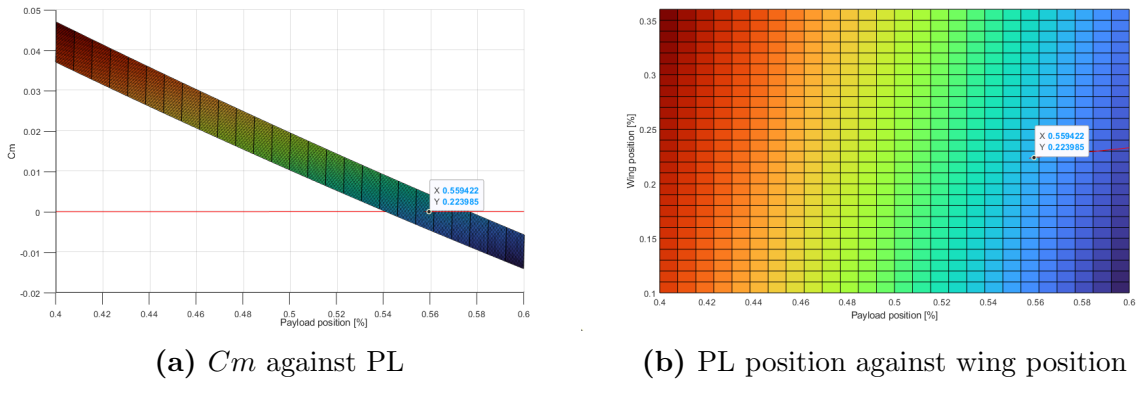


Figure 26: Different points of view from figure 25.

Taking into account all the conditions mentioned before, it was selected the configuration marked in Figure 25, due to the fact that $C_{m\alpha} = 0$ and $C_m = -0.001$. So, it can be concluded that in order to have the mentioned pitching moments it has to be set $x = 0.56$, $y = 0.22$ and $Tail_{pos}$ at 82% of the fuselage.



12.2 Roll momentum

The roll coefficient plays a decisive role in a competition. This coefficient is very important because it will determine how fast an aircraft will roll given a specific angle of the aileron deflection, δ_a .

The roll control and stability can be expressed as Equation 48 shows.

$$C_L = C_{L_0} + C_{L_\beta} \beta + C_{L_{\delta_a}} \delta_a + C_{L_{\delta_r}} \delta_r \quad (48)$$

Where C_{L_β} takes control of the stability in the presence of a β disturbance, $C_{L_{\delta_a}}$ and $C_{L_{\delta_r}}$ are the control coefficients, related with the δ_a and δ_r variations, and C_{L_0} term that focuses on the roll momentum due to the aircraft geometry. Note that β is the yaw angle, δ_a and δ_r are the angle deflected by the ailerons or the rudder, respectively.

In this section, it will only be studied the $C_{L_{\delta_a}}$. It is important to set up positive variations of angles and momentum. In this case, it is going to be positive when the left aileron deflects to the landing gear, therefore the right aileron deflects to the opposite side. The positive direction of roll momentum will be from the CG of the airplane to the rotor.

For the purpose of calculating this coefficient, some assumptions have to be done:

- ◊ Ailerons are considered plane flaps.[31]
- ◊ Aileron deflection of $\delta_a = 15^\circ$ entails a lift increment of $\Delta C_l = 0.2$.[31]
- ◊ No losses for tip wing are being considered.
- ◊ In order to simplify the calculation, the Cl distribution along the wingspan was considered linear.

In order to achieve this coefficient, it is going to be calculated the lift distribution along the wingspan, Figure 27a and 27b, and the momentum distribution, Figure 28a and 28b. After several iterations, it was selected to fix ailerons of 30% of half of the wingspan and its center suited at the 75% of half wingspan referred from the center line of the aircraft.

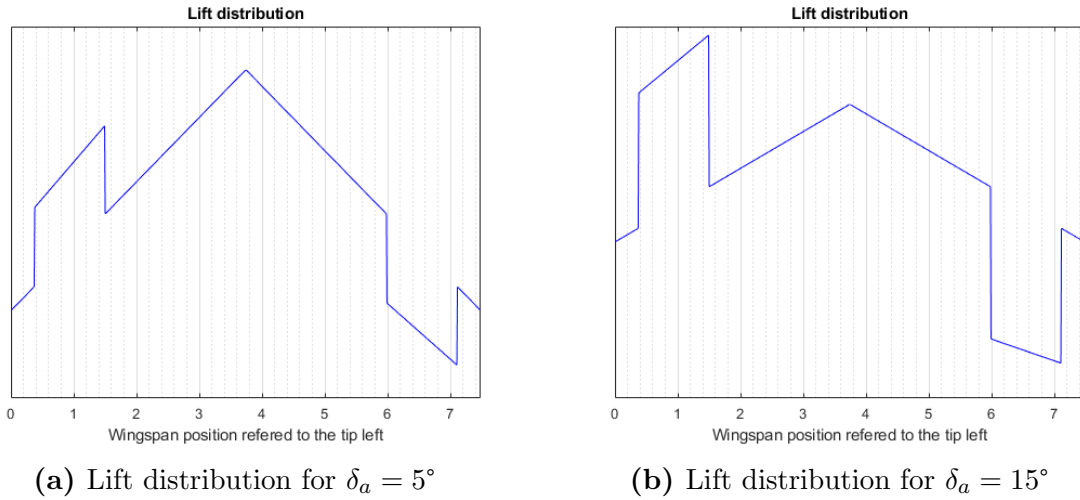


Figure 27: Lift distribution along the wing.

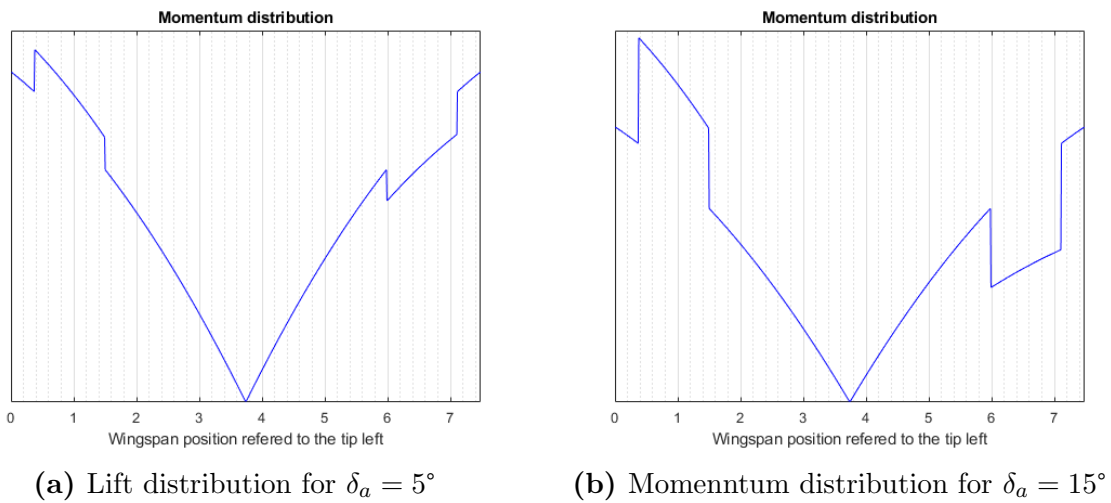


Figure 28: Momentum distribution along the wing.

It is important to notice that Figure 28a and 28b are not a momentum diagram from structure theory, it is the torque generated in each elementary node, showing that the more lift is applied higher momentum is reached.

For instance, for the Figure 28b case, it is obtained a total momentum of 3624 Nm .

Using the basic equation of the inertia momentum, equation 49.

$$\tau = I\alpha \quad (49)$$

Where τ is the momentum, I is the moment of inertia and α is the angular acceleration. The moment of inertia considering only the wings is $I = \sum_{n=1}^n m_i x_i^2 = 2 \cdot (40 \cdot (b/4)^2)$. So,



replacing the values in equation 49, $\alpha = 12.95 \text{ rad/s}^2$. Considering that this acceleration is applied for 0.1 s in this time the aircraft has gained an angular speed of $\omega = 1.29 \text{ rad/s} \approx 74^\circ/\text{s}$.

Despite the approximations made, this result seems to be accurate due to the fact that this type of aircraft must fast roll turns in order to have good performance in competitions.

Calculating the roll coefficient momentum for each angle deflection, considering that there is a linear relationship between the flap deflection and the lift increment ($\Delta C_l = \frac{0.2}{15} \delta_a$). It is obtained that $C_{L\delta_a} = 0.0013$, which seems to be very small, however, it can not be compared with other aircraft because there is not much information about this specific coefficient. One of the reasons that might be causing this is the number of coefficients that equation 48 has so that the contribution of all the parameters should not result in a high value of C_L .

13 Fuselage design

The fuselage is a critical part to determine during the design of an aircraft. Several computational analysis techniques are usually used to determine the lightest configuration capable of handling the maximum stresses. However, in this project, the fuselage design will not be studied in much detail.

As a reference aircraft to design Voltic's fuselage, the EXTRA 300 L and the Sbach 342 were used. Both have rectangular sections for the lower part of the fuselage. As it can be seen in Figure 29, the upper part consists of an arch that starts at the back of the pilot and ends at the rear tip of the fuselage. It is used the cockpit glass as a junction of the rear arch with the fuselage front surfaces. The geometry used for the cockpit glass is commonly used in this type of aircraft. This shape helps to improve visibility when demanding maneuvers are being done. The nose has two lateral air entries for cooling the propulsion system.

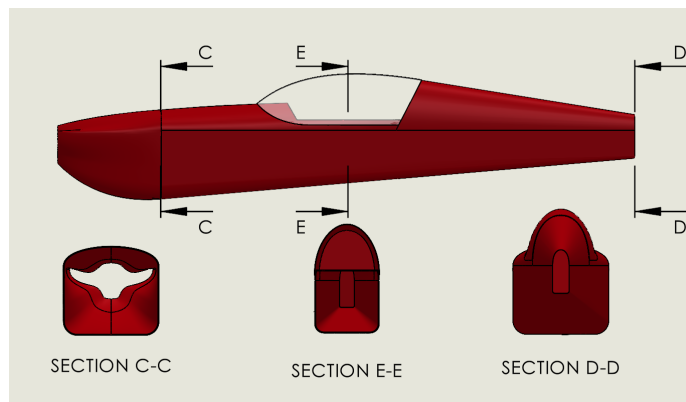


Figure 29: Fuselage concept design.

The full length of the fuselage is 7.02 meters. This result is obtained using a method proposed by Sadraey's book [1] (Table 6.2), which uses the distance between the tail and the wing.

13.1 Landing Gear

As it was mentioned in previous sections, it is going to use a fixed landing gear with an external fairing. This type of landing gear was selected in order to support the landing forces and not complicate the mechanism, but without compromising aerodynamics.

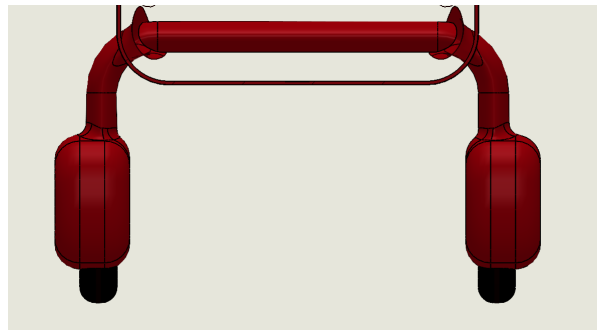


Figure 30: Front view: Landing gear concept design.

The structure consists of an internal structural part and an external firing part, thus improving the aerodynamics of the assembly. The fairing has a teardrop profile as shown in Figure 31.

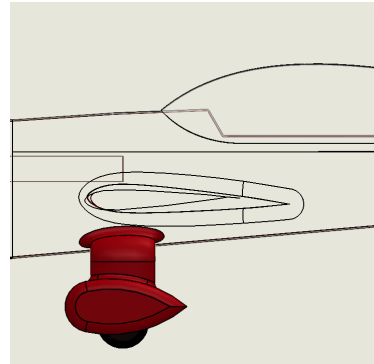


Figure 31: Lateral view: Landing gear concept design.



14 Renders and drawings

In this section some drawings and reders of Voltic are going to be shown. In these renders and drawings some data of geometric and general parameters of the final result of this preliminary design can be found.

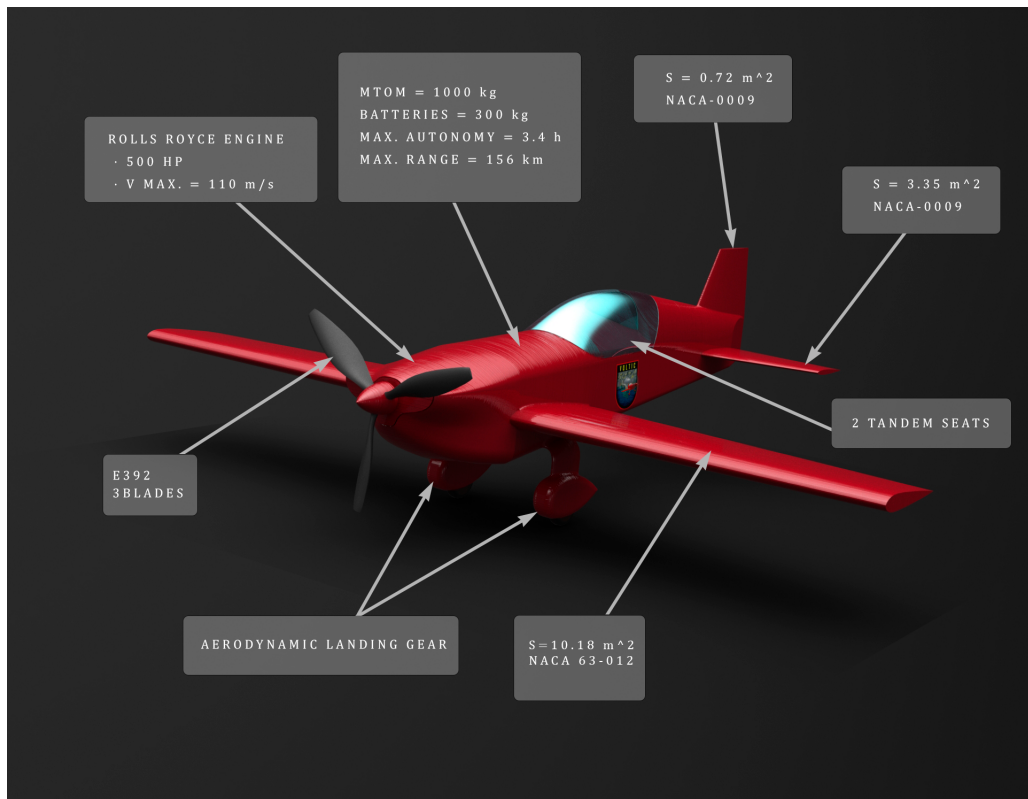


Figure 32: General information of Voltic.

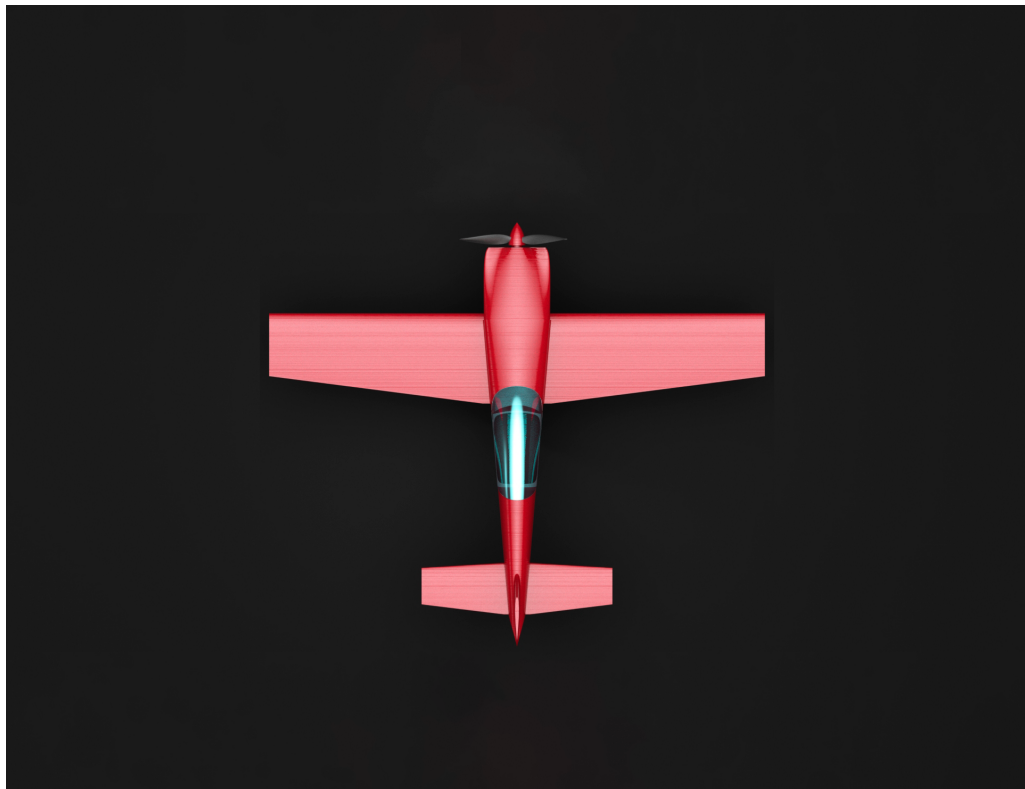
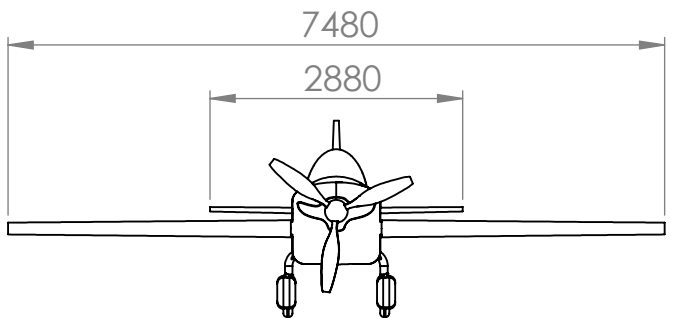


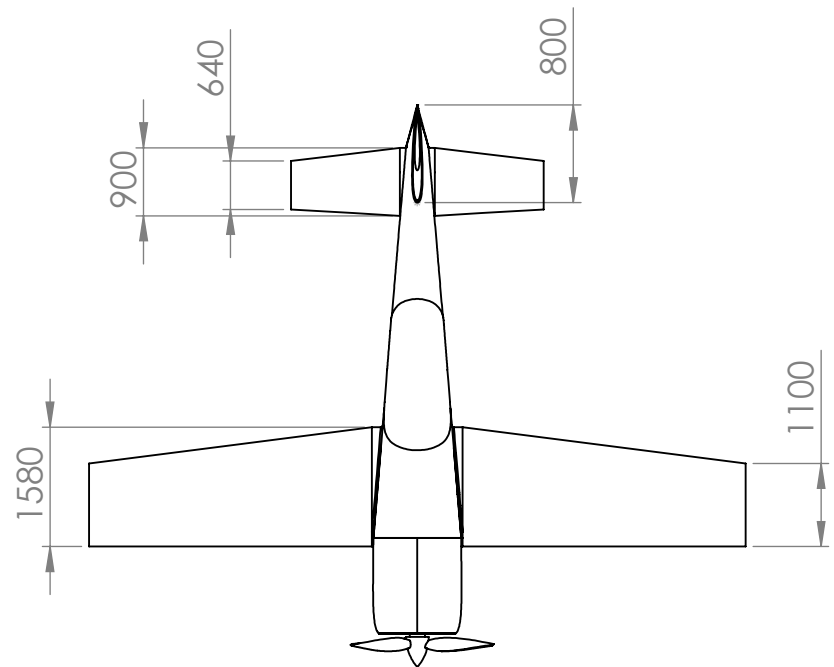
Figure 33: Plan view of voltic.

6 5 4 3 2 1

D



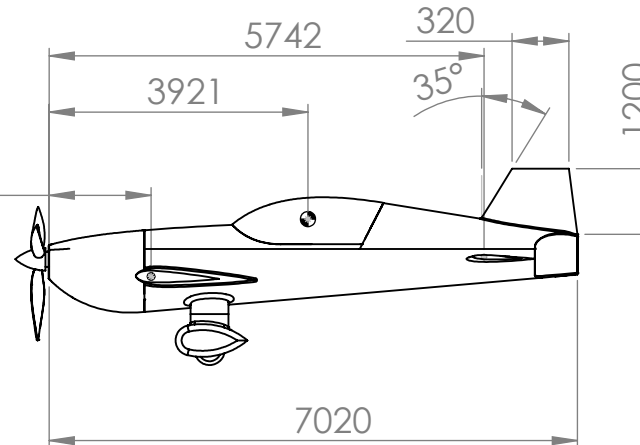
C



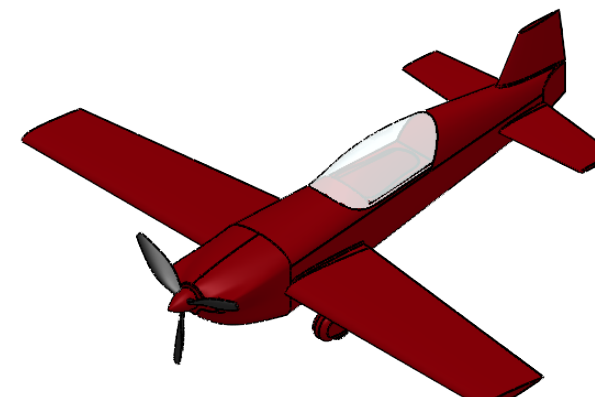
3 2 1

D

1540



C



B

TITLE:	VOLTIC PLANE	REVISION	1
DRAWING NAME	voltic_aerobatic_plane		
SCALE:	1:100		
PAGE 1 OF 1	A4 28/12/22		

A



15 Conclusions

At the beginning of this project, some Top Level Requirements (*TLR*) were set in order to demand an aircraft capable of meeting its needs while reducing its environmental footprint. Once all the analysis and calculations have been done, it is concluded that four out of the five *TLR* have been accomplished.

In section 8, Electric propulsion, it was proven that the maximum aircraft autonomy driven by an electric engine is **3.4 h** and at cruise speed is **1.2 h**, 240% more than the initial minimum required, 0.5 h. Once the wing design was done at 10, Wing design, and with the data collected in 8, Electric propulsion, it has been shown that the plane can take off at **200 m** without the necessity of designing high lift aerodynamics devices, which greatly simplified the calculations.

Finally, in section 13, Fuselage design, a two-seater aerobatic fuselage has been designed. Nevertheless, as it is shown in section 7, Maneuver and gust diagram, due to CS-23 regulations a g force threshold of +8g, -5g has not been achieved. Instead, the aircraft will be able to handle **+5.5g, -3.5g**, which is an acceptable result for a preliminary design. In future phases of the design, a more detailed study could be made on the structural strength to withstand the 8g.

This way, in this first preliminary design, quite favorable results have been obtained. Hence, it is believed that it could be feasible to advance the design of this conceptual aircraft.



References

- [1] Mohammad H Sadraey. *Aircraft design: A systems engineering approach*. John Wiley & Sons, 2012.
- [2] Raphael Hallez, Claudio Colangeli, Jacques Cuenca, and Laurent de Ryck. Impact of electric propulsion on aircraft noise – all-electric light aircraft case study. 07 2018.
- [3] Portal Movilidad [Online]. Motores eléctricos vs a combustión ¿quién gana? [Accessed: 14 December 2022]. Available in: <https://portalmovilidad.com/motores-electricos-vs-a-combustion-quien-gana-nuevo-informe-de-amech-compara-los-puntos-mas-importantes/>.
- [4] Inc AVSTAR Aircraft of Washington. So how many G's can my plane take? [Accessed: 28 December 2022]. Available in: https://www.avstarair.com/ask_mike/ask_mike_archive/03-07-1999.htm, 2022.
- [5] Royal Aeronautical Society. Can you design an all-electric aerobatic aircraft? [Accessed: 28 September 2022]. Available in: <https://www.aerosociety.com/news/can-you-design-an-all-electric-aerobatic-aircraft/>, 2022.
- [6] Aviation Heroes. Peter Besenyei's display under the bridges of Budapest. [Accessed: 28 September 2022]. Available in: <https://www.youtube.com/watch?v=KOFsfMY7IPc>, 2022.
- [7] Bart Hoekstra [Online]. The Xtremeair sbach 342. [Accessed: 26 September 2022]. Available in: <https://www.airhistory.net/photo/264089/D-ETXA>.
- [8] Extra Aerobatic Planes [Online]. The Extra330LE made its first flight. [Accessed: 20 September 2022]. Available in: https://www.extraaircraft.com/news.php?quale_news=39&lang=4&tipo=&tutte=.
- [9] Rolls-Royce Limited [Online]. ‘spirit of innovation’ stakes claim to be the world’s fastest all-electric vehicle. [Accessed: 2 October 2022]. Available in: <https://www.flickr.com/photos/rolls-royceplc/albums/72157705298410174>.
- [10] [Online]. ‘extra ea-300. [Accessed: 14 December 2022]. Available in: https://en.wikipedia.org/wiki/Extra_EA-300.
- [11] [Online]. La fuerza aérea argentina subasta sus aviones acrobáticos sukhoi su-29. [Accessed: 14 December 2022]. Available in: <https://www.zona-militar.com/2021/05/05/la-fuerza-aerea-argentina-subasta-sus-aviones-acrobaticos-sukhoi-su-29/>.
- [12] AOPA [Online]. Evaluating experimental aircraft. [Accessed: 14 December 2022].



Available in: <https://www.aopa.org/news-and-media/all-news/2020/june/pilot/evaluating-experimental-aircraft>.

- [13] Annette J. Carson [Online]. Aerobatics. [Accessed: 25 September 2022]. Available in: <https://www.britannica.com/sports/aerobatics>.
- [14] Anonymous [Online]. Barnstorming. [Accessed: 2 October 2022]. Available in: <https://en.wikipedia.org/wiki/Barnstorming>.
- [15] Anonymous [Online]. Fédération aéronautique internationale. [Accessed: 2 October 2022]. Available in: https://en.wikipedia.org/wiki/F%C3%A9d%C3%A9ration_A%C3%A9ronautique_Internationale.
- [16] Anonymous [Online]. Fai world aerobatic championships. [Accessed: 2 October 2022]. Available in: https://en.wikipedia.org/wiki/FAI_World_Aerobatic_Championships.
- [17] Airline Cost Management Group (ACMG) [Online]. [Accessed: 25 September 2022]. Available in: https://www.iata.org/contentassets/3b5a413027704ce08976fe1890fb43e2/acmg_highlights.pdf.
- [18] CAE Global Academy [Online]. Airline and business jet pilot demand outlook 10-year view, 2020 update. [Accessed: 25 September 2022]. Available in: <https://www.cae.com/cae-pilot-demand-outlook-2020/CAE-Pilot-Demand-Outlook-2020.pdf>.
- [19] United States of America [Online] Federal Aviation Administration (FAA). Aircraft weight and balance control. technical report ac 120-27f. [Accessed: 7 December 2022]. Available in: https://www.faa.gov/documentLibrary/media/Advisory_Circular/AC_120-27F.pdf.
- [20] Aviation Performance Solutions [Online]. weight of extra300l. Available in: <https://apstraining.com/aircraft/extra-300l/>.
- [21] Lycoming [Online]. Operator's manual lycoming aeio-320, aeio-360 aeio-540 series. Available in: <https://www.lycoming.com/sites/default/files/AEIO-320-360-540%20per%20Manual%2060297-21.pdf>.
- [22] Danie P. Raymer. *Aircraft Design: A Conceptual Approach*. AIAA Education Series, 1989.
- [23] EASA [Online]. CS-23. [Accessed: 18 November 2022]. Available in: <https://www.easa.europa.eu/en/downloads/1742/en>, 2012.
- [24] Helmut Schenk. Propeller calculator. Available in: <http://www.drivecalc.de/PropCalc/>.



-
- [25] Ester Comellas. *Apunts de Disseny d'Avions*. 5 september 2022.
 - [26] Yasa Limited [Online]. 750r electric motors product sheet. [Accessed: 22 November 2022]. Available in: <https://www.yasa.com/wp-content/uploads/2021/05/YAS-A-750RDatasheet-Rev-11.pdf>.
 - [27] Airfoiltools. [Accessed: 10 December 2022]. Available in: <http://airfoiltools.com/>.
 - [28] Douglas Aircraft Company. *USAF stability and control datcom*. University of Michigan Library, 1975.
 - [29] Andrew Wood. Sweep Angle and Supersonic Flight. [Accessed: 28 December 2022]. Available in: <https://aerotoolbox.com/intro-sweep-angle/>, 2022.
 - [30] Panagiotis Kefalas, Dionissios Margaris, Marios Drossos, and Ioannis Spyropoulos. Conceptual design of an aerobatic trainer aircraft. June 2018.
 - [31] Tousif Ahmed, Md. Tanjin Amin, S. Islam, and Shabbir Ahmed. Computational study of flow around a naca 0012 wing flapped at different flap angles with varying mach numbers. *Global Journal of Researches in Engineering*, 13, 01 2013.



Appendices

A Code

A.1 OEM & MTOM estimation

This code fits a linear regression of OEM against MTOM using the reference aircraft.

```

1 %%LINEAR REGRESSION
2 MTOM=[ 850 1100 737 952];
3 OEM=[ 670 760 521 628];
4
5
6 coeff=polyfit (MTOM, OEM,1) ;
7 syms x
8 f=coeff(1)*x + coeff(2);
9
10 fpplot(f, [0 1200], 'color', "b")
11 ylim([0 1000])
12 hold on
13
14 plot(MTOM, OEM, 'O', 'MarkerSize',5, 'color', "k")
15 ylabel("OEM [Kg]")
16 xlabel("MTOM [Kg]")
17 title("Linear regression between OEM & MTOM")
18 grid on
19 grid minor
20
21 plot(757,557, '.', 'MarkerSize',20, 'color', "r")
22 plot(1000,704, '.', 'MarkerSize',20, 'color', "g")
23 hold off
24 legend('Linear regression', 'Reference aircraft points',
25 'Approximated point', 'Corrected point', 'Location', 'northwest')
```

A.2 Performance diagram

This code shows the performance diagram of Voltic using an adaptation of Sadraey's method, by setting different restrictions. Finally, it is done a plot with all the restrictions to visualize which is the design area of Voltic.

```

1 clc
2 close all
3 clear
4 %% Variable definition
5
6 Density_SL=1.225;
```



```

7 Density=1.07;
8 Density_C=0.863; %h_c=3500 m (service)
9 Sigma=Density/Density_SL ;
10 Sigma_C=Density_C/Density_SL ;
11 g=9.8;
12 V_stall=30;
13 CL_max=2;
14 V_max=98;
15 AR=5.5;
16 CD_0=0.03;
17 Propeller_eff=0.8;
18 Fiction_coeff=0.04; %Asphalt
19 e=0.88; %0.65 - 0.8
20 K=1/(pi*e*AR);
21 S_TO=200;
22 k_TO=1.2;
23 V_TO=k_TO*V_stall;
24 CL_flapTO=0.5; %0.3 - 0.8
25 CL_C=0.3; %CL cruise
26 CL_TO=CL_C+CL_flapTO;
27 CD_0LG=0.008; %0.006 - 0.012
28 CD_0HLD_TO=0.005; %0.003 - 0.008
29 CD_0TO=CD_0+CD_0LG+CD_0HLD_TO;
30 CD_TO=CD_0TO+K*CL_TO^2;
31 CD_G=CD_TO-Fiction_coeff*CL_TO;
32 CL_R=CL_max/k_TO^2;
33 ROC=12.7;
34 ROC_C=0.508;
35 L_D_max=10;
36
37 %% Equations
38 syms W_S_s W_S_Vmax W_S_TO W_S_ROC W_S_h %W_P_Vmax W_P_TO W_P_ROC
39 %W_L_h y_aux
40
41 W_S_s=0.5*Density*V_stall^2*CL_max;
42
43 W_P_Vmax=Propeller_eff/(0.5*Density_SL*V_max^3*CD_0*1/W_S_Vmax+(2*K*
    W_S_Vmax)/(Density*Sigma*V_max));
44
45 W_P_TO=((1-exp(0.6*Density*g*CD_G*S_TO*W_S_TO^-1))/(Fiction_coeff-((
    Fiction_coeff+CD_G/CL_R)*exp(0.6*Density*g*CD_G*S_TO*W_S_TO^-1))))*
    Propeller_eff/V_TO;
46
47 W_P_ROC=1/(ROC/Propeller_eff+(sqrt((2/(Density*sqrt(3*CD_0/K)))*W_S_ROC)*
    (1.155/(L_D_max)*Propeller_eff)));
48

```



```

49 W_P_h=Sigma_C/(ROC_C/Propeller_eff+(sqrt((2/(Density_C*sqrt(3*CD_0/K)))*
    W_S_h)*(1.155/(L_D_max)*Propeller_eff)));
50
51 %% Plots
52 f1=solve(W_P_Vmax,W_S_Vmax);
53
54
55 fplot(W_P_TO,[0 2000],':','Color','r','LineWidth',1);
56 hold on;
57 fplot(W_P_Vmax,[0 2000],'—','Color',[0.4660 0.6740 0.1880]','LineWidth',
    1);
58 hold on;
59 fplot(W_P_ROC,[0 2000],'-.','Color','b','LineWidth',1);
60 hold on;
61 fplot(W_P_h,[0 2000],'—',[0.4940 0.1840 0.5560]','LineWidth',1)
    ;
62 hold on;
63 xline(W_S_s,"Color",'k','LineWidth',1);
64 hold on;
65 yline(0.026284,' ':'Color','m','LineWidth',1)
66 hold on;
67 yline(0.037786,' ':'Color','b','LineWidth',1)
68 ylim([0 0.15]);
69
70 scatter(904.57,0.037786,"blue","filled");
71 scatter(741.1011,0.03549,"red","filled");
72 %[xout,yout]=intersections(W_P_Vmax,W_P_h);
73 W_S=W_S_s;
74 WP=0.026284;
75 scatter(W_S_s,WP,"green","filled");
76 legend('Take-off','V max','ROC','Ceiling','V Stall',
    'Rolls-Royce Engine','Extra 330LE Engine','Extra 330LE',
    'Sbach 342','Design point');
77 xlabel('W/S [N/m^2]');
78 ylabel('W/P [N/W]');
79 title('Performance diagram');
80
81 hold off;
82
83
84 %% Surface calculation
85
86
87 MTOM=1000;
88 MTOW=MTOM*g;
89 S=MTOW/W_S;
90 Power=MTOW/(W_P*745.7);
91 display(S);

```



```

92 display(Power);
93 display(W_S);
94 display(W_P);

```

A.3 Drag coefficients estimation

This code computes a preliminary estimation of the aircraft drag polar. It does not have any particular function or algorithm. Its objective is to facilitate the calculations and plot the respective polar curve.

```

1 function [CD,S,P]=drag(WTO)
2
3 %% Some Constants
4
5 Density=1.07;
6 Density_SL=1.225;
7 Density_C=0.863; %h_c=3500 m (service)
8 Sigma=Density/Density_SL;
9 AR=5.5;
10 Propeller_eff=0.8;
11 e=1.78*(1-0.045*AR^0.68)-0.64;
12 Vc=81.67; %Cruise velocity m/s
13 V_stall=30;
14 V_max=1.2*Vc;
15 WS_d=963; %Wing loading of the design point
16 WP_d=0.026284; %Power loading of the design point
17 C_l_HLD = 0.4; %High lift devices lift contribution
18
19 S = WTO/WS_d;
20 P = WTO/WP_d;
21 Wavg = WTO; %Our weight is constant
22 W = WTO; %Our weight is constant
23
24
25 C_Lc = (2*Wavg)/(Density_C*Vc^2*S); %Aircraft ideal cruise
26 %lift coefficient
27 C_Lcw = C_Lc/0.95; %Wing cruise lift coefficient
28 C_li = C_Lcw/0.9; %Wing airfoil ideal lift coefficient
29
30 C_Lmax = (2*WTO)/(Density_SL*V_stall^2*S); % Aircraft maximum
31 %lift coefficient
32 C_Lmax_w = C_Lmax/0.95; %Wing maximum lift coefficient
33 C_lmax_gross = C_Lmax_w/0.9; %Wing airfoil gross maximum lift coefficient
34
35 C_lmax = C_lmax_gross - C_l_HLD;
36
37

```



```
38 %Drag coefficients estimation
39 k = 1/(pi*e*AR);
40 CD0 = (2*P*Propeller_eff/V_max -(4*k*W^2)/(Sigma*V_max^2*S)) / (Density_SL*
41 V_max^2*S);
42 Message=strcat('CD = ',num2str(CD0), '+', num2str(k), '*CL^2');
43 %disp(Message)
44
45 CL = -3:0.1:3;
46 CD = [CD0 k];
47
48 % plot(CL,CD0+k*CL.^2);
49 % title('Aircraft Polar');
50 % xlabel('CL');
51 % ylabel('CD');
52 % ax = gca;
53 % ax.XAxisLocation = 'origin';
54 % ax.YAxisLocation = 'origin';
55 % grid on;
56 end
```

A.4 Maneuver and gust diagram

This code shows the aerodynamic loads that the aircraft will support during a flight with and without wind, by following the regulation CS-23 [23]. Finally, it is shown two plots to visualize these two situations.

```
1 clc
2 close all
3 clear
4
5 W_S=963; %N/m^2
6 W_S_ft=W_S/47.8803; %lbs/ft^2
7 Vc_kts=36*sqrt(W_S_ft); %kts
8 Vc_min=Vc_kts/1.94384; %m/s
9 Vc=Vc_min;
10 Vd=1.55*Vc_min;
11 Vs=30;
12 n=8;
13 n_min=-5;
14 Va=Vs*sqrt(n);
15 S=10.1765;
16 CL_min=-1.2;
17 Vs_neg=sqrt((-1000*9.81)/(0.5*1.225*CL_min*S));
18 Va_neg=Vs_neg*sqrt(abs(n_min));
19
20 nf=2;
```



```

21 CL_max_TO=2.5;
22 Vf_1=sqrt ( nf*1000*9.81/(0.5*1.225*S*CL_max_TO) );
23 VsF=sqrt ( 1000*9.81/(0.5*1.225*S*CL_max_TO) );
24 Vf=max(1.8*VsF,1.4*Vs);
25
26 Vb_gust=20.11;
27 Vc_gust=15.24;
28 Vd_gust=7.62;
29
30 AR=5.5;
31 e=0.88;
32 CLalpha=2*pi/(1+2*pi/(pi*e*AR));
33 nb=1+(1.225*Vb_gust*CLalpha*Va)/(2*W_S);
34 nc=1+(1.225*Vc_gust*CLalpha*Vc)/(2*W_S);
35 nd=1+(1.225*Vd_gust*CLalpha*Vd)/(2*W_S);
36 nb_neg=1-(1.225*Vb_gust*CLalpha*Va)/(2*W_S);
37 nc_neg=1-(1.225*Vc_gust*CLalpha*Vc)/(2*W_S);
38 nd_neg=1-(1.225*Vd_gust*CLalpha*Vd)/(2*W_S);
39
40 x1=linspace (0 ,Va,1000);
41 y1=0.00111111*x1.^2;
42 x1_aux=linspace (0 ,Va,10000);
43 y1_aux=0.00111111*x1_aux.^2;
44 x3=linspace (0 ,Va_neg,1000);
45 y3=-(x3/Vs_neg).^2;
46 x4=linspace (0 ,Va,10000);
47 y4=1-(1.225*Vb_gust*CLalpha*x4)/(2*W_S);
48 y5=1+(1.225*Vb_gust*CLalpha*x4)/(2*W_S);
49 xf=linspace (0 ,Vf_1,1000);
50 yf=0.0015884572519376*xf.^2;
51
52 Intersect=abs(y1_aux-y4);
53 for i=1:10000
54 if Intersect ( i )<5*10^-4
55 P=([x4(i) y4(i)]);
56 end
57 end
58
59 Intersect2=abs(y1_aux-y5);
60 for i=1:10000
61 if Intersect2 ( i )<6*10^-4
62 P1=([x4(i) y5(i)]);
63 end
64 end
65
66 x6=linspace (P(1) ,P1(1) ,1000);

```



```

67 y6=0.001111111*x6.^2;
68
69 %% figure 1
70 grayColor1 = [.5 .5 .5];
71 plot(x1,y1, Color='blue');
72 hold on;
73 plot([Va Vd], [n n], Color='blue');
74 plot(x3,y3, Color='blue');
75 plot([Vd Vd], [n 0], Color='blue');
76 plot([Va_neg Vc], [n_min n_min], Color='blue');
77 plot([Vc Vd], [n_min 0], Color='blue');
78 plot(xf,yf, Color='red');
79 plot([Vf_1 Vf], [nf nf], Color='red');

80
81 plot([Vs Vs], [0 1], 'Color', grayColor1, LineStyle='—');
82 text(Vs+1, 0.5, 'V_s_1','FontSize',8);
83 plot([Vf Vf], [0 nf], 'Color', grayColor1, LineStyle='—');
84 text(Vf+1, 1, 'V_f','FontSize',8);
85 plot([Va Va], [0 n], 'Color', grayColor1, LineStyle='—');
86 text(Va+1, 3.5, 'V_a','FontSize',8);
87 plot([Vc Vc], [n_min n], 'Color', grayColor1, LineStyle='—');
88 text(Va_neg-1, -2, 'V_s_-1','HorizontalAlignment','right','FontSize',8);
89 plot([Va_neg Va_neg], [n_min 0], 'Color', grayColor1, LineStyle='—');
90 text(Vc+1, 1, 'V_c','FontSize',8);
91 text(Vd+1, 3.5, 'V_d','FontSize',8);
92 plot([0 Vd], [0 0], 'Color', grayColor1);
93 grid on;
94 xlabel('V (m/s)');
95 ylabel('n');
96 ylim([-6 9]);
97 title('Maneuver diagram at sea level')

98
99
100
101 %% figure 2
102 figure;
103 Int=8175;
104 plot(x1,y1, Color='blue');
105 hold on;
106 plot([Va Vd], [n n], Color='blue');
107 plot(x3,y3, Color='blue');
108 plot([Vd Vd], [n 0], Color='blue');
109 plot([Va_neg Vc], [n_min n_min], Color='blue');
110 plot([Vc Vd], [n_min 0], Color='blue');

111
112 grayColor = [.6 .6 .6];

```



```

113 plot([0 P1(1)], [1 P1(2)], 'Color', grayColor, LineStyle='—');
114 plot([0 P1(1)], [1 y4(Int)], 'Color', grayColor, LineStyle='—');
115 %plot([0 Va], [1 nb_neg], 'Color', grayColor, LineStyle='--');
116 plot([P1(1) P1(1)], [y4(Int) P1(2)], 'Color', grayColor, LineStyle='—');
117
118 plot([0 Vc], [1 nc], 'Color', grayColor, LineStyle='—');
119 plot([0 Vc], [1 nc_neg], 'Color', grayColor, LineStyle='—');
120 plot([Vc Vc], [nc_neg nc], 'Color', grayColor, LineStyle='—');
121
122 plot([0 Vd], [1 nd], 'Color', grayColor, LineStyle='—');
123 plot([0 Vd], [1 nd_neg], 'Color', grayColor, LineStyle='—');
124 plot([Vd Vd], [nd_neg nd], 'Color', grayColor, LineStyle='—');
125
126 text(P1(1)+1, 1, 'V_b', 'FontSize', 8);
127 text(Vc+1, 1, 'V_c', 'FontSize', 8);
128 text(Vd+1, 1, 'V_d', 'FontSize', 8);
129
130 plot([P1(1) Vc], [P1(2) nc], Color='red', LineWidth=1);
131 plot([Vc Vd], [nc nd], Color='red', LineWidth=1);
132 plot([Vd Vd], [nd nd_neg], Color='red', LineWidth=1);
133 plot([Vc Vd], [nc_neg nd_neg], Color='red', LineWidth=1);
134 plot([P1(1) Vc], [y4(Int) nc_neg], Color='red', LineWidth=1);
135 plot(x6,y6, Color='red', LineWidth=1);
136 plot([P(1) P1(1)], [P(2) y4(Int)], Color='red', LineWidth=1);
137 %plot([P(1) Va], [P(2) nb], Color='red', LineWidth=1);
138 grid on;
139 xlabel('V (m/s)');
140 ylabel('n');
141 ylim([-6 9]);
142 title('Gust diagram at sea level')

```

A.5 Electric Propulsion

This code takes as inputs four airspeed velocities and their respective engine revolutions. By using the software PropCalc [24] the corresponding propeller thrust and power are obtained, for each airspeed velocity to engine revolution ratio. Thereafter, the program computes the thrust and power coefficients which are used to obtain the propeller-engine and engine-battery performances. Finally, it calculates the flight time and the range of Voltic.

```

1 clc
2 close all
3 clear
4
5 drag = @Aero;
6
7 % Inputs

```



```

8 v_inf = [49.9 69.1 81.9 97.9]; %Poner en m/s
9 n_H = [3000 3000 3000 3000]/60; %Poner en rpm
10 T = [6840.701 4801.205 3185.577 911.42];% Obtener de PropCalc
11 P_H = [476529.8 394651.7 294287.6 110237.8];% Obtener de PropCalc
12 D = 2.030; %m
13 Density_C=0.863; %h_c=3500 m (service)
14 WIO=1000*9.81; %Maximum take off weight
15
16 % Parametros fabricante
17 i0 = 0.006; % A
18 Kv = 0.25; %
19 Re = 10; % Ohms
20
21 rt = 1; % Relacion de transmision
22
23 % Vectors
24 J = zeros(4,length(v_inf));
25 C_T = zeros(1,length(n_H));
26 C_PH = zeros(1,length(n_H));
27
28 Thrust_coeff = zeros(1,length(v_inf));
29 Power_coeff = zeros(1,length(v_inf));
30
31 % Calculations
32 for i=1:length(v_inf)
33     C_T(i) = (T(i)/(Density_C*D^2*(n_H(i)*D)^2));
34     C_PH(i) = (P_H(i)/(Density_C*pi*D^2*(n_H(i)*D)^3));
35     for k=1:length(v_inf)
36         J(k,i) = (v_inf(i)/(n_H(i)*D))^(k-1);
37     end
38 end
39
40 J_inv = inv(J);
41
42 Thrust_coeff = C_T*J_inv;
43 Power_coeff = C_PH*J_inv;
44
45 % A6.1 Empenta i veolcitat de vol coneudes
46 V_stall=30;
47 Power_frac=zeros(1,82+10-V_stall);
48 tiempo=zeros(1,82+10-V_stall);
49 v_inf_vec=zeros(1,82+10-V_stall);
50 distance=zeros(1,82+10-V_stall);
51 for v_inf=V_stall:1:82+10
52 cont=0;
53 [CD,S,P] = drag(WIO);

```



```

54
55 T = 0.5*Density_C*v_inf^2*CD(1)*S + (CD(2)*WTO^2)/(0.5*Density_C*v_inf^2*S)
      ; % VRU
56
57 a = [ Thrust_coeff(1) v_inf*Thrust_coeff(2) v_inf^2*Thrust_coeff(3)-(T/(
      Density_C*D^2)) v_inf^3*Thrust_coeff(4) ];
58 r = roots(a); %r=n_H*D
59
60 P_H = zeros(1,length(r));
61 n_H = zeros(1,length(r));
62
63 for i=1:1:length(r)
64   if r(i)>0
65     P_H(i) = Density_C*D^2*r(i)^3*Power_coeff(1) + Density_C*v_inf*
      D^2*r(i)^2*Power_coeff(2) + Density_C*v_inf^2*D^2*r(i)*
      Power_coeff(3) + Density_C*v_inf^3*D^2*Power_coeff(4);
66     n_H(i) = r(i)/D;
67     w_H(i) = 2*pi*n_H(i);
68     Q_H(i) = P_H(i)/w_H(i);
69     eta_H(i) = (T*v_inf)/(Q_H(i)*w_H(i));
70
71     w_m(i) = rt*w_H(i);
72     Q_m(i) = Q_H(i);
73     eta_rt(i) = (Q_H(i)*w_H(i))/(Q_m(i)*w_m(i)); % = (1/rt)
74     P_m(i) = P_H(i)/eta_rt(i); % = P_H *r
75
76     V(i) = Q_m(i)*Re*Kv + w_m(i) +i0*Re;
77     I(i) = Q_m(i)*Kv + i0 ;
78     Power=V(i)*I(i);
79     cont=cont+1;
80     if cont==1
81       Power_frac(1,v_inf-V_stall+1)=Power;
82     else
83       if Power_frac(1,v_inf-V_stall+1)>Power && Power>0
84         Power_frac(1,v_inf-V_stall+1)=Power;
85       end
86     end
87     eta_m(i) = (Q_m(i)*w_m(i))/(V(i)*I(i));
88   else
89     r(i)=0;
90   end
91 end
92 tiempo(1,v_inf-V_stall+1)=300*250/Power_frac(1,v_inf-V_stall+1);
93 distance(1,v_inf-V_stall+1)=tiempo(1,v_inf-V_stall+1)*v_inf;
94 v_inf_vec(1,v_inf-V_stall+1)=v_inf;
95 end

```



```

96
97 plot(v_inf_vec, tiempo);
98 xlim([30 92])
99 xlabel(['V_{Cruise} [m/s]', 'Fontsize', 12]);
100 ylabel(['t [h]', 'Fontsize', 12]);
101 grid on
102 title("Flight time (V_{Cruise}))")
103 figure
104 plot(v_inf_vec, distance);
105 xlim([30 92])
106 xlabel(['V_{Cruise} [m/s]', 'Fontsize', 12]);
107 ylabel(['R [km]', 'Fontsize', 12]);
108 grid on
109 title("Range (V_{Cruise}))")

```

A.6 Range vs payload

This code is useful to calculate the Voltic's range depending on some parameters like the payload.

```

1 PL = 200;
2 MTOM= 800+PL;
3 M_bat=300;
4 m=M_bat/MTOM;
5 v=51;
6 n=1.34;
7 EF=0.64;
8 E=250*3600;
9 g=9.8;
10 RO=1.225;
11 S=10.18;
12
13
14 L=MTOM*g*n;
15 C_L=L/(RO*(v^2)*S/2);
16 C_D=0.048379+0.065418*(C_L^2);
17 D=C_D*RO*(v^2)*S/2;
18 AE=L/D;
19
20 R = (m*AE*E*EF/g)/1000;

```

A.7 Stability and control

This code first calculates the center of gravity with symbolic values. Then compute the center of gravity depending on the position of PL and wing's position. Finally, it is calculated the momentum coefficient, and the line where $C_{m\alpha} = 0$. Also, several plots are done during the process to visualize the results.



```

1 %%MASS CENTER REFERENCED FROM TIP OF THE AIRCRAFT
2 clear
3 %close all
4 clc
5
6 %%
7 pos_PL=linspace (0.4 ,0.6 ,27) ;
8 %pos_PL_aux=linspace (0.4 ,0.6 ,17) ;
9 [ ~ ,k]=size ( pos_PL ) ;
10 syms y
11 pos=0.10:0.01:0.36;
12 [ ~ ,m]=size ( pos ) ;
13 Moment_coeff=zeros ( k ,m ) ;
14 for j=1:k
15
16     x = pos_PL(1,j) ;
17     L_fus=7.02;
18     l_opt=4.22;
19     m_engi_bat=325;
20     PL=200;
21     m_wing=80;
22     m_tail=20;
23     tail_pos=(l_opt/L_fus+y);
24     m_fuss=1000 - m_wing - m_engi_bat - PL;
25     X_cg = ( L_fus*(m_engi_bat*0.2 + PL*x+ m_wing*y + 0.25*m_fuss + m_tail*
26         tail_pos)) / 1000;
27
28 figure
29 hold on
30 grid on
31 grid minor
32
33 CL_w=0.26;
34 eta_h=0.9;
35 Sh=2.25;
36 Sw=10.18;
37 V_H=0.7;
38 h_0=0.39/L_fus; %centre aerodynamic - LE
39 h=h_0-(y-X_cg/L_fus); %LE-CG
40 CL_h=CL_w*(h-h_0)/(eta_h*V_H);
41 for i=1:m
42     v=rand (3,1) ;
43     pos_wing=pos(1,i) ;
44     tail_pos_i=double (subs (tail_pos ,y ,pos_wing )) ;

```



```

45 %%{
46     a=m_engi_bat/10;
47     b=0.01*i-0.01;
48     plot(0.125,b,'.', 'MarkerSize',a, 'color', v)
49
50     a=m_fuss/10;
51     plot(0.25,b,'.', 'MarkerSize',a, 'color', v)
52     a=PL/10;
53
54     plot(x,b,'.', 'MarkerSize',a, 'color', v)
55     a=m_wing/10;
56     plot(pos_wing,b,'.', 'MarkerSize',a, 'color', v)
57     a=5;
58     plot(tail_pos_i,b,'.', 'MarkerSize',a, 'color', v)
59 %}
60 X_cg = ((m_engi_bat*0.2 + PL*x+ m_wing*pos_wing + 0.25*m_fuss +
61           m_tail*tail_pos_i) / 1000);
62 plot(X_cg,b,'o', 'MarkerSize',5, 'color', "k")
63
64 Moment_coeff(j,i)=CL_w*( X_cg-pos_wing)-eta_h*(Sh/Sw)*double(subs(
65           CL_h,y, pos_wing))*(tail_pos_i-X_cg);
66
67 end
68 end
69 CL_w_alpha=4.44;
70 AR=2/3 * 5.5;
71 e=1.78*(1-0.045*AR^0.68)-0.64;
72 CL_h_alpha=2*pi/(sqrt(1+(2/AR)^2)+2/AR);
73 syms x_prima y_prima
74 tail_pos_prima=(l_opt/L_fus+y_prima);
75 X_cg_alpha = ((m_engi_bat*0.2 + PL*x_prima+ m_wing*y_prima + 0.25*m_fuss +
76           m_tail*tail_pos_prima) / 1000);
77 eq=solve(CL_w_alpha*( X_cg_alpha-y_prima)-eta_h*(Sh/Sw)*CL_h_alpha*(
78           tail_pos_prima-X_cg_alpha)==0,y_prima);
79 %}
80 figure
81 surf(pos_PL, pos, Moment_coeff)
82 hold on
83 xlim([0.4 0.6])
84 ylim([0.1 0.36])
85 fplot(eq, 'color', "r")

```

This code first computes the lift distribution along the wingspan, then the momentum elementary distribution along the wingspan. Finally, calculation of the momentum coefficients are done.



```

1 %CONTROL CODE
2 clc
3 clear
4 close all
5 %Defining geometry
6 syms y
7 angle=0:1:15;
8 [~,m]=size(angle);
9 Cm=zeros(1,m);
10 for j=1:m
11     DeltaCl=angle(1,j)*0.2/15;
12     c_root=1.58;
13     c_tip=1.1;
14     b=7.48;
15     chord=2*(c_root/2+(c_tip-c_root)/(b)*(y-b/2));
16     V=82; %m/s
17     rho=0.7048;
18     percent=0.6;
19     n=100;
20     delta_x=(b/2)/n;
21     nodes_right=zeros(1,n);
22
23     for i=1:n
24         if i==1
25             nodes_right(1,1)=delta_x/2+b/2;
26         else
27             nodes_right(1,i)=nodes_right(1,i-1)+delta_x;
28         end
29     end
30
31 Roll_moment=zeros(1,n);
32 Mid_chord=zeros(1,n);
33 surface=zeros(1,n);
34 Lift=zeros(1,n);
35 for i=1:n
36     Cl=0.4877;
37     a=nodes_right(1,i);
38     if a>(percent*b/2+b/2) && a<(0.9*b/2+b/2)
39         Cl=Cl-DeltaCl;
40     end
41
42     Mid_chord(1,i)=double(subs(chord,y,a));
43     surface(1,i)=(double(subs(chord,y,a+delta_x/2))+double(subs(chord,y,a-
44         delta_x/2)))*delta_x/2;
45     Lift(1,i)=rho*V^2*Cl*0.5*surface(1,i);
        Roll_moment(1,i)=(nodes_right(1,i)-b/2)*Lift(1,i);

```



```

46
47     end
48
49
50 %LEFT
51 nodes_left=zeros(1,n);
52 for i=1:n
53     if i==1
54         nodes_left(1,1)=delta_x/2;
55     else
56         nodes_left(1,i)=nodes_left(1,i-1)+delta_x;
57     end
58 end
59
60
61 Roll_moment_left=zeros(1,n);
62 Mid_chord_left=zeros(1,n);
63 surface_left=zeros(1,n);
64 Lift_left=zeros(1,n);
65 chord_left=2*(c_tip/2+(c_root-c_tip)/(b)*(y));
66 for i=1:n
67     Cl=0.4877;
68     a=nodes_left(1,i);
69     if a<((1-percent)*b/2) && a>((1-0.9)*b/2)
70         Cl=Cl+DeltaCl;
71     end
72     Mid_chord_left(1,i)=double(subs(chord_left,y,a));
73     surface_left(1,i)=(double(subs(chord_left,y,a+delta_x/2))+double(subs(
74         chord_left,y,a-delta_x/2)))*delta_x/2;
75     Lift_left(1,i)=rho*V^2*Cl*0.5*surface_left(1,i);
76     Roll_moment_left(1,i)=(b/2-nodes_left(1,i))*Lift_left(1,i);
77 end
78 sum(Lift_left)
79 plot(nodes_left,Roll_moment_left,'color','b')
80 hold on
81 plot(nodes_right,Roll_moment,'color','b')
82 xlim([0 b])
83 Tot_moment=sum(Roll_moment_left)-sum(Roll_moment);
84 Inertia=2*(40*(b/4)^2);
85 angular_acc=Tot_moment/Inertia;
86
87 set(gca,'YTick',[])
88 grid on
89 grid minor
90 title("Momentum distribution")
91 xlabel("Wingspan position refered to the tip left")

```



```
91 figure
92 plot(nodes_right , Lift , 'color' , "b")
93 hold on
94 plot(nodes_left , Lift_left , 'color' , "b")
95 grid on
96 grid minor
97 set(gca , 'YTick' ,[])
98 title("Lift distribution")
99 xlabel("Wingspan position refered to the tip left")
100 xlim([0 b])
101 Cm(1,j)=Tot_moment/(0.5*rho*10.18*V^2*b);
102 end
```



B Velocities calculation

This section shows how the velocities for the flight envelope have been calculated. First of all, the operations used are all extracted from CS-23 [23], so the results respect the restrictions imposed by the regulation.

The first speed to calculate is the cruise speed (V_c), whose formula, for an aerobatic plane is the following one.

$$V_c = 36 \sqrt{\frac{W}{S}}$$

Where the velocity is in knots and the wing loading is in lb/ft^2 . So, to compute V_c in SI, it has to be applied the conversion factor for both parameters. To change from N/m^2 to lb/ft^2 , it has to be divided by 47.88, and from *kts* to *m/s*, it has to be divided by 1.944.

$$V_c = \frac{36}{1.944} \sqrt{\frac{W/S}{47.88}} = 85 \text{ m/s}$$

The design dive speed (V_d) is the absolute maximum speed the aircraft can fly, it is even greater than the maximum speed. For an aerobatic airplane:

$$V_d = 1.55 V_c = 129 \text{ m/s}$$

Next, the design maneuvering speed (V_A). This speed depends on the stall speed (V_s), which has been calculated earlier, in section 5.

$$V_A = V_s \sqrt{n_{max}} = 84 \text{ m/s}$$

Moreover, the maneuvering speed in the negative range of the load factor (V_{s-1}) has to be calculated too. It works the same way but using the negative parameters of the aircraft. In this case $V_{stall(neg)}$ is 36 m/s and V_{s-1} is:

$$V_{s-1} = V_{stall(neg)} \sqrt{n_{min}} = 80 \text{ m/s}$$

Finally, there are two ways to compute the maximum speed with the flaps fully extended (V_F), and it will be taken the greater between both speeds. The first way is to take V_s and multiply it by 1.4, and the second method is to compute the stall speed with the flaps fully extended ($V_{SF} = 25 \text{ m/s}$) and multiply it by 1.8.

- ◊ Method 1: $V_F = 42 \text{ m/s}$



◊ Method 2: $V_F = 45 \text{ m/s}$

So, V_F is computed by method 2.